Time Arrow Spinors for the Modified Cosmological Model

Jonathan W. Tooker
Occupy Numbers, Dates, and Times
(Dated: 7/26/2018)

We construct time arrow spinor states and define for them a Stern–Gerlach analogue Hamiltonian. The dispersion relations of the allowed modes are derived in a few special cases. We examine experimental data regarding negative frequency resonant radiation and show that the energy shift of the negative frequency mode is on the characteristic scale of the energies of the new Hamiltonian. We describe the similitude of the modified cosmological model (MCM) and the Stern–Gerlach apparatus, and we also show how the Pauli matrices are well-suited to applications in MCM cosmology. Complex and quaternion phase are combined in the wavefunction to generate new multiplectic structures. The principles described in this paper are oriented toward a time circuit application so we briefly describe an electrical circuit whose constructive elements elucidate the requirements needed for a working time circuit. The algebraic graph representation of electrical nodes with different electric potentials is replaced with time nodes that have different times in the time circuit graph.

TIME ARROW SPINORS

To obtain a cosmological role for the Pauli matrices, we will consider that time in the MCM should be described with spinors. This follows from [1, 2] wherein we proposed that the x^0 of x^μ spacetime should be taken as the superposition of two time components. For this application we will write $x^0 \equiv t_\star$ or $\chi^5_\varnothing \equiv t_\star$ [3] and say that $t_\star$ is the superposition of $t_\pm$, as in figure 1. In this way, we derive an analogy with a generalized spin-1/2 state being written as the superposition of spin-up and spin-down eigenstates. The idea to define a superposition time first arose in response to a question raised by Ashtekar and Singh in reference [4]. They wrote,

> "Can we extract, from the arguments of the wave function, one variable which can serve as *emergent time* with respect to which the other arguments evolve? Such an internal or emergent time is not essential to obtain a complete, self-contained theory. But its availability makes the physical meaning of dynamics transparent and one can extract the phenomenological predictions more easily. In a pioneering work, DeWitt proposed that the determinant of the 3-metric can be used as internal time [5]. Consequently, in much of the literature on the Wheeler-DeWitt (WDW) approach to quantum cosmology, the scale factor is assumed to play the role of time, although sometimes only implicitly. However, in closed models the scale factor fails to be monotonic due to classical recollapse and cannot serve as a global time variable already in the classical theory. Are there better alternatives at least in the simple setting of quantum cosmology?"

As a simple superposition of $t_\pm$, $t_\star$ may or may not contain the requisite freedom such that all other dynamical quantities can evolve with respect to it. The DeWitt emergent time can be used as an effective emergent time in non-closed models but it contains nothing more than

was in 3-metric so it cannot be a truly emergent, globally functional emergent time. Likewise with $t_\star$, as a superposition it is constrained to contain not more information than was in its constructive elements. However, later in this paper we will show that $t_\star$ is, indeed, fully dynamical and contains more information than is in $t_\pm$. This will depend on a lattice construction whose global phase relationships are constrained by a normalization condition on $t_\star$. The lattice construction will be such that $t_\pm$ can each individually be taken as $t'_\star$ which is the superposition of some other $t'_\pm$. Those, in turn, can be labeled $t''_\star$ and decomposed as $t''_\pm$, and on and on, such that the phase and magnitude of everything in the lattice is eventually constrained by the way it will contribute to the normalized top-level $t_\star$. In this way, $t_\star$ will be an emergent time with respect to which *all* of the other arguments evolve.

DeWitt has shown [5] that the determinant of the 3-metric can be used as an emergent time in certain limiting conditions. Therefore, consider the always Euclidean 3-spaces in $\Sigma^\pm$ [6] spanned by $\chi^a_\pm$ with $a \in \{2, 3, 4\}$. These spaces are identically flat in the chirological metrics $\Sigma^\pm_{ab}$ [7] but they are de Sitter (dS) and anti-de Sitter (AdS) spaces in the chronological metrics $g^\pm_{ij}$. Therefore, while they both evolve with the same $t_\star \equiv x^0$, we may construct two distinct $t_\pm$ with $\det g^\pm_{ij}$ because g^-_{ij} is the spatial part of anti-de Sitter space and g^+_{ij} is the spatial part of de Sitter space. In turn, when we use $t_\pm$ to con-
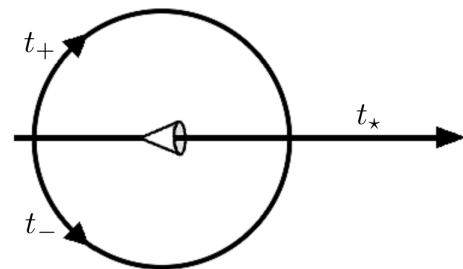

FIG. 1. This figure demonstrates that time $t_\star$ is the superposition of two time components $t_\pm$.

struct $t_\star \equiv \chi_\varnothing^5$, either as a sum, tensor product, or other operation, they will have unequal contributions. This reflects the original comments regarding figure 1: the system supports a parity violating field theory due to the due the separation of a closed interior region from an exterior open neighborhood of transfinite infinity [6, 8–11]. In this paper, we will consider the non-relativistic limit without asymmetrical contributions from dS and AdS.

The MCM superposition time $t_\star$ was constructed in response to the question posed by Ashtekar and Singh but the construction has its own independent physical motivations. These were first described in [1] and are described at length in [2]. Restated here: consider some universe U created in a big bang. All of the p_i momenta in that universe are conserved with respect to the zero momentum that existed before the big bang, *i.e.*: the momentum of the part of U moving to the left is equal to the momentum of the part moving to the right, and the same for the forward/backward and up/down spatial dimensions. However, the p_0 part of the 4-momentum is positive-definite in U when time always increases in magnitude [12] or, equivalently, in the convention where binding energy is always negative. Since this quantity p^0 is positive-definite everywhere in U, it has nothing negative to balance it out. This contrasts the p^i momenta wherein a galaxy floating to the left has negative momentum with respect to a galaxy floating to the right.

Where did this anomalous increment of 4-momentum $p^0 > 0$ come from and why did the universe decide not to conserve momentum at the big bang? While ΛCDM cosmology is quite happy to violate the law conservation of momentum, we do not do so in the MCM. Therefore, let two universes U and $\bar{U}$ originate in the big bang singularity, not just one. The time axes of these universes are $t_\pm$ such that t_+ increases in the opposite direction to the increase of t_-. Since time flows in the opposite direction in $\bar{U}$, the ADM positive-definiteness theorem [12], and all other theorems demonstrating the positive-definiteness of p^0, will show that the p^0 component of the 4-momentum of $\bar{U}$ is negative-definite. Combining U and $\bar{U}$, the MCM system conserves momentum and is, therefore, obviously better than ΛCDM, in every conceivable way, at all times. *N.b.*: we have derived a requirement for $\bar{U}$ following exactly that logical deduction which led Pauli to hypothesize neutrinos.

The only *modification* that the MCM makes to the ΛCDM cosmological model is to let there be two universes that strictly conserve momentum instead of a single universe which does not conserve momentum at its origin. Since one universe is behind the CMB with respect to the other one, there is little reason to think that the presence of the second universe would disrupt the ΛCDM description of the first. As an exception to this generality, we have demonstrated that the gravity of the second universe can lead to dark energy effects in the first [1, 2, 13]. Therefore, where dark energy is a mystery in ΛCDM, it is not a mystery in the MCM. Likewise, the polarization of the multipole moments of the CMB are not explained in ΛCDM yet they may be derived in the

MCM through the symmetry axis between U and $\bar{U}$.

Through conservation of momentum we derive two times $t_\pm$ pointing in opposite directions from the big bang. We obtain the superposition time $t_\star$ from $t_\pm$ via a quantum mechanical argument: the observer is unable to determine if he is in the universe with forward time or backward time. To an observer in either universe, time in that universe is forward and the other is backward. This is in complete analogy with quantum mechanical spin: if the quantum observer cannot determine whether a two-state spin system is in the spin-up or spin-down eigenstate then he must write the state as a superposition

$$|\psi_\pm\rangle = c_\uparrow |\uparrow\rangle + c_\downarrow |\downarrow\rangle \ . \tag{1}$$

Adapting from electron to universe, we write

$$|t_\star\rangle = c_+ |t_+\rangle + c_- |t_-\rangle \ . \tag{2}$$

with eigenspinors

$$|t_+\rangle = \begin{pmatrix} 1 \\ 0 \end{pmatrix} \ , \quad \text{and} \quad |t_-\rangle = \begin{pmatrix} 0 \\ 1 \end{pmatrix} \ . \tag{3}$$

We are well-motivated to apply this principle of superposition in the cosmological setting because the MCM uses the two universes U and $\bar{U}$ as two quanta of spacetime. If U is a particle then $\bar{U}$ is its anti-particle and the big bang was an ordinary field fluctuation. Incidentally, we also use this construction to shed light on the imbalance in the universe of the ratio of baryons to anti-baryons [13]. U has a positive baryon number B and $\bar{U}$ has a negative baryon number $-B$ so that the MCM cosmology is baryon neutral, as expected but not evident in ΛCDM. It is only when ΛCDM decides to throw out the law of conservation of momentum that the anomalous non-zero baryon number is observed.

In the original formulation of the MCM, the bounce only happened at the big bang. As the model developed, the bounce was moved to the singular present moment instead of some singularity long ago and far away. The reasoning for this change appeared in [1] and is thus: if $t_\star$ is a superposition of $t_\pm$ then we must be able to decompose it into its fundamental pieces at $t_\star = t_0$, not only at $t_\star = 0$. The MCM unit cell, figure 2, embodies the concept of a singularity in every moment when there is an interaction with a singularity $\varnothing$ between every two adjacent moments of physical time $\mathcal{H}_1$ and $\mathcal{H}_2$. When each unit cell contains a singularity, that makes it completely clear what it means to move the big bang, or the big bounce, from the beginning of the universe into any given moment. The MCM unit cell only describes U at the bounce and, in the present study, we want to include U and $\bar{U}$, as in figure 3. Figure 3 shows two universes going through a simultaneous big bounce rather than having a common origin in a non-bouncing big bang [13]. While we will work with representations
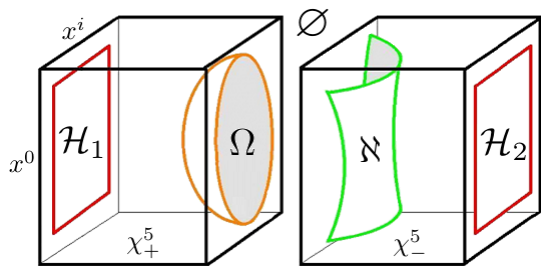
FIG. 2. In each transit of the unit cell of the MCM cosmological lattice, the trajectory along χ^5 "bounces" off of a singularity of infinite curvature at $\varnothing$. $\mathcal{H}_1$ and $\mathcal{H}_2$ are two adjacent moments of a single universe and in this paper we will consider two universes moving oppositely through time, both bouncing off the same singularity $\varnothing$.
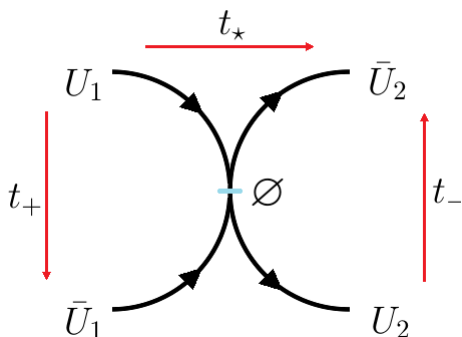

FIG. 3. This figure shows the directions of the arrows of the three primary time components. U evolves forward in both $t_\star$ and t_+, and $\bar{U}$ evolves forward in $t_\star$ and t_-, which is to say that $\bar{U}$ evolves backwards in t_+. U_1 and U_2 are like the $\Sigma^\pm$ that appear in figure 2.

like figure 3 in this paper, the inclusion of $\varnothing$ in figure 2 gives a good motivation for bouncing: the $\varnothing$ singularity can't be a big bang because $\mathcal{H}_1$ precedes it.

$\Sigma^\pm$ are joined on a topological singularity [10, 14], but general relativity says that topological singularities are black holes which should capture geodesics from Σ^+ without continuing them into Σ^-. As a fine point, if χ^5_- is opposite time with respect to χ^5_+ then the singularity is a white hole in Σ^- and we are well-motivated to consider the extension of the trajectory through $\varnothing$ as per usual in the Penrose diagram of a black hole. Indeed, one might build a condition of identical topological flatness in the bulk [6, 11] through the superposition of a black hole and a white hole, or a pair of singularities of infinite positive and negative curvature.

Another point that must be addressed before moving on is the reconciliation of the different time schemes in figures 1 and 3 relative to that in figure 2. For the purposes of this paper, we will work in the convention of figure 3 but the rectangular unit cell of figure 2 neither shows x^0 leading to $\varnothing$, as in figure 3, nor does it show $t_\pm$ meeting up with $t_\star$ twice, as in figure 1. On the latter, if the $\chi^5_\pm$ of figure 2 continue into adjacent unit cells then they will meet $\mathcal{H}$ a second time, and we can

write off the discrepancy to the non-circular resolution of the periodic boundary condition. Insofar as figure 2's x^0 does not lead to $\varnothing$, if we take χ^5_+ pointing to $\varnothing$ as $t_\star$ then we can take $\pm x^0$ as the $t_\pm$ components. Here we refer to the concept mentioned above that every time component must have a $t_\star$ representation as the superposition of $t_\pm$ pieces. Indeed, the dynamical objects of general relativity are 3-spaces and we must be allowed to propagate them along the x^0 or χ^5_+ directions without disrupting the structure of the theory. Taking χ^5_+ as $t_\star$ is fully self-consistent when the momentum of the universe evolving with $+x^0$ is exactly offset by the momentum obtained from the universe evolving with $-x^0$ normalized such that p^0 is negative-definite there. Note how the concept of *infinite complexity* [1] is demonstrated when every time piece has a $t_\star$ representation as the sum of $t_\pm$ contributions.

PAULI MATRICES

Consider the Pauli matrices

$$\mathbb{I} \equiv \hat{\sigma}_0 = \begin{pmatrix} 1 & 0 \\ 0 & 1 \end{pmatrix} \tag{4}$$

$$\hat{\sigma}_1 = \begin{pmatrix} 0 & 1 \\ 1 & 0 \end{pmatrix} \tag{5}$$

$$\hat{\sigma}_2 = \begin{pmatrix} 0 & -i \\ i & 0 \end{pmatrix} \tag{6}$$

$$\hat{\sigma}_3 = \begin{pmatrix} 1 & 0 \\ 0 & -1 \end{pmatrix} \quad . \tag{7}$$

Before we examine how the well-known algebra of spin-1/2 should be extended to our time arrow spinors, we should examine the Pauli matrices at their most fundamental level. They are like a complexified superset of the 2D permutation matrices, of which there are only two:

$$P_1 = \begin{pmatrix} 1 & 0 \\ 0 & 1 \end{pmatrix} \quad , \qquad \text{and} \qquad P_2 = \begin{pmatrix} 0 & 1 \\ 1 & 0 \end{pmatrix} \quad . \tag{8}$$

P_1 is the identity, which we write as $\hat{\sigma}_0$, and $\hat{\sigma}_1 = P_2$. $\hat{\sigma}_2$ is like P_2 with some extra phase and $\hat{\sigma}_3$ is like P_1 with some extra phase. If we are to interpret the Pauli matrices as complexified permutation matrices, which is what they plainly are at the most fundamental level of linear algebra, then it begs the question: permutations of what?

To begin, consider the time arrow conventions for $\{t_-, t_\star, t_+\}$ in figure 3. The eventual aim in this representation, beyond the scope of this paper, would be to construct a cosmological time circuit akin to that which can be solved with linear algebra in the way that one solves Kirchoff's laws in an electrical circuit. The complete circuit would have many instances of the bounce

complex, figure 3, joined horizontally and vertically, and the "law" enforced by the algebra would be that there is a path somewhere in the circuit of forward flowing time in a state of unitarity. One might notice that such a circuit would always contain exterior legs connected to more bounce complexes, but we would invoke the MCM principle that considers at most three simultaneous levels of ℵ [6, 8–10]. This would constrain the diagram not to extend out infinitely when we exclude legs too far removed from the top-level $t_\star$ path.

In figure 3, the universe U moves forward in time according to both $t_\star$ and t_+, and $\bar{U}$ moves in reverse time with respect to t_+ and forward with respect to $t_\star$ and its own time t_-. If we put $\bar{U}$ moving backward with respect to $t_\star$ then it would move forward in t_+. That might be acceptable but it is not the convention that we will consider here. Naively, when a U plane wave is incident on the bounce from the top left, it can only come out on the bottom right leg of the the diagram because of the forward-only time evolution conditions on $t_\star$ and t_+ individually. However, when the MCM includes dynamical process proportional to the advanced and retarded times [15], we must consider backscattering through time, into the other universe. Therefore, we will consider that the probability density incident on the bounce from U_1 can scatter into any of the other three legs. We should not consider backscattering along the U_1 leg because of the forward-only time evolution condition in any given universe. Anything moving backward along U_1 must have originated in $\bar{U}$ and presently we consider only a source in U_1 moving toward $\varnothing$. Since $\varnothing$ is a singularity of both infinite positive curvature and infinite negative curvature, it is not outlandish to consider that time gets mixed up when two topologically independent universes scatter there. In [16], we discussed the mixing of timelike and spacelike components of $e^{i(\omega t - kx)}$ at the boundary of $\Sigma^\pm$ as relates to their respective O(1,4) and O(2,3) topologies, and if we add an extra universe built on $\check{\Sigma}^\pm$ then we will have even more channels for mixing. Spacelike and timelike regions are usually separated by a conformally invariant lightlike region [17] but these topological sectors are merged in $\varnothing$ due to the infinite curvature.

Plane waves are like bosons and we need to develop the MCM spinor component whose origin was independently motivated in [18]. Since a universe is more like a matter particle than a force-carrying particle, it should be fermionic in nature, *i.e.*: spinor-valued. The time arrow spinor defined along each leg of the bounce complex (figure 4) will tell us how $t_\star$ transforms across the bounce. Therefore, consider a spinor wave $\Psi = e^{ikx}|t_\star\rangle$ incident on the bounce from U_1. We take e^{ikx} as totally generic and not referring specifically to one coordinate sector of the MCM unit cell or another, and we condense $\omega t - kx$ into the 4-vector notation kx. With a spinor in place, we should examine what the Pauli matrices do to it. Before we do that, let us examine figure 4 and make a prediction based on purely physical motivations. For obvious reasons, we have assigned $\hat{\sigma}_0 \equiv \mathbb{I}$ to the U_1

leg. What about the others? If we want our initial state in the $t_\star$ channel to be fully specified by U_1 then we should make the $\bar{U}_1$ piece imaginary with the $\hat{\sigma}_2$ matrix. This gives a sector of $t_\star$ leading into the bounce which is completely determined by U_1 even while $\bar{U}_1$ exists in a parallel sector. Our $t_\pm$ spinors are eigenstates of the $\hat{\sigma}_3$ matrix and, therefore, we should assign $\hat{\sigma}_3$ to the U_2 leg. If we start with t_+ or t_- in U_1, and then nothing happens as it moves from $\mathcal{H}_1$ to $\mathcal{H}_2$, we need to get that same state out, and that requires that it be an eigenstate of the operator that sends it to U_2. By default, we have no choice but to attach $\hat{\sigma}_1$ to the $\bar{U}_2$ leg.

With our physically motivated expectations defined, we write the total set of operations as

$$\hat{\sigma}_0|t_\pm\rangle = |t_\pm\rangle \tag{9}$$
$$\hat{\sigma}_1|t_\pm\rangle = |t_\mp\rangle \tag{10}$$
$$\hat{\sigma}_2|t_\pm\rangle = \pm i|t_\mp\rangle \tag{11}$$
$$\hat{\sigma}_3|t_\pm\rangle = \pm|t_\pm\rangle \tag{12}$$

As expected, $|t_\pm\rangle$ are eigenspinors of $\hat{\sigma}_3$ but not $\hat{\sigma}_1$ or $\hat{\sigma}_2$. If $t_\star$ is incident on the bounce, $t_\star$ being some combination of $t_\pm$, and it comes out on the $\hat{\sigma}_3$ leg, as in equation (12), then the t_+ component has moved forward in time and the t_- component has moved in the opposite direction to increasing t_-, thus the -1 eigenvalue. If it comes out on the $\hat{\sigma}_1$ or $\hat{\sigma}_2$ legs, then $t_\pm \to t_\mp$. This condition will imply that the timewave has left the universe and gone into the other universe whose time arrows are reversed with respect to the first one. On the $\hat{\sigma}_1$ leg, $t_\star$ continues to increase so there is no sign or phase change attached to the swapped components. For scattering into the $\hat{\sigma}_2$ leg, the wave has to begun to propagate oppositely through $t_\star$ and oppositely with respect to the forward flowing time t_- of $\bar{U}$. Therefore, the $\bar{U}_1$ leg must be imaginary to circumvent the forward-only time law in the top-level $t_\star$. Overall, when we put a superposition of $t_\pm$ in, we will always get a superposition of $t_\pm$ out. In the special case when $t_\pm$ have equal coefficients in $|t_\star\rangle$, then $|t_\star\rangle$ is an eigenspinor of $\hat{\sigma}_1$ so that case deserves special attention.

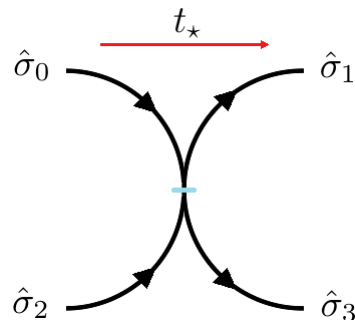There is an interpretive difficulty with $t_\star$ along the U_2

FIG. 4. This figure shows how the Pauli matrices $\hat{\sigma}_i$ assign the permutations of the time arrows along the three possible exits.

leg because $|t_\star\rangle$ is not an eigenspinor of $\hat{\sigma}_3$ even while $|t_\pm\rangle$ are. The U_1 state that entered the bounce was

$$|t_\star\rangle = c_+|t_+\rangle + c_-|t_-\rangle \quad , \tag{13}$$

but, using equation (12), the state that exits the bounce along U_2 is

$$\hat{\sigma}_3|t_\star\rangle = c_+|t_+\rangle - c_-|t_-\rangle \quad . \tag{14}$$

Therefore, the proposed process does not preserve a static $t_\star$ ground state. To develop a solution, note that where the bounce complex is clearly amenable to circuit analysis, the four-legged bounce configuration was proposed in [13] in no small part because it is amenable to analysis in QFT. The bounce complex is like a Feynman diagram with four legs meeting at a vertex. A typical rule in diagrammatic QFT is that one must consider all permutations of a given diagram. Therefore, switch one of figure 4's legs around to get figure 5. The rearranged scheme of figure 5 is very much like figures 6 and 7 which first appeared in [2] to describe the decomposition of $t_\star$ into its $t_\pm$ components within the bulk of the unit cell. Indeed, the $\hat{\sigma}_2$ leg is the imaginary piece and, in [2], we showed that figure 6 should be like figure 7 wherein the non-$\mathcal{H}$ bulk of the unit cell is imaginary. This is also well-aligned with the definition for complex numbers $z = x^0 \pm i\chi_\pm^5$ [10] which translates roughly as $z = t_\star \pm it_\pm$.

Using the identity that $\hat{\sigma}_2^2 = \mathbb{I}$, we can apply $\hat{\sigma}_2$ to the imaginary $\hat{\sigma}_2$ leg of figure 5 to preserve Ψ across a double bounce via

$$\hat{\sigma}_2^2|t_\star\rangle = |t_\star\rangle \quad . \tag{15}$$

This fixes the signage problem of equation (14). Indeed, where we have a curved leg on the left of figure 5, we might replace that with a straight leg and say that it is the superposition of $t_\pm$ components from U_1 and $\bar{U}_1$. As we have operated on the $\hat{\sigma}_2$ leg with $\hat{\sigma}_2$ to demonstrate the imaginary throughput, we could likewise achieve this by applying $\hat{\sigma}_1$ to the $\hat{\sigma}_1$ leg or $\hat{\sigma}_3$ to the $\hat{\sigma}_3$ leg because all of the Pauli matrices have the property $\hat{\sigma}_\mu^2 = \mathbb{I}$. However, where the $\hat{\sigma}_1$ and $\hat{\sigma}_3$ legs will meet other bounce complexes in a more complex circuit, as in figure 8, the imaginary $\hat{\sigma}_2$ channel will not.

Figure 8 brings us back to the question raised by Ashtekar and Singh about the construction of an emergent time. Superficially, one might argue that a superposition time adds nothing new but figure 8 shows how the $t_\star$ path can be used to normalize all other time arrows in the lattice. Whatever the interactions are, $t_\star$ needs to be preserved with unchanging coefficients for $t_\pm$. Physically, this represents the normalization of the 4-velocity which causes time to pass always at the same rate in an inertial frame. While figure 8 is only a qualitative description, it defines the mechanism by which one path through the time circuit will be the "emergent
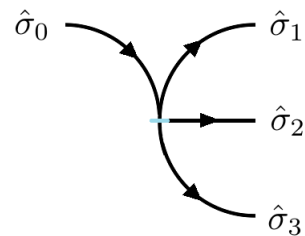

FIG. 5. In this figure, the imaginary phase of $\hat{\sigma}_2$ is used to go into the bulk space between $t_\pm$. This operation is well-suited to be such that the operand of $\hat{\sigma}_i$ is in $\mathcal{H}$ and the output in the bulk of the MCM unit cell. Here we have the potential to inflate a unit cell without having to evolve across it as $\vec{\sigma}_i \rightarrow \{\hat{2}, \hat{\Phi}, \hat{i}\}$.
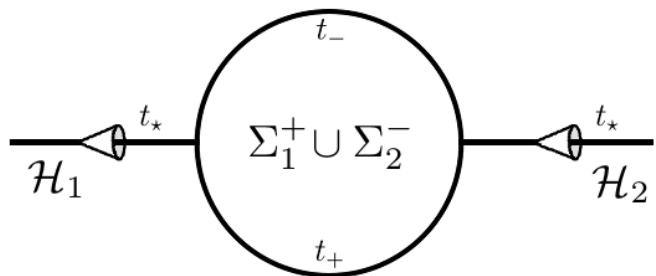

FIG. 6. This figure demonstrates the decomposition of $t_\star$ in $\mathcal{H}$ into its spinor basis components during transit of the unit cell. Note that where figure 3 is like the the QFT diagram of two particle scattering, this figure is like a photon decaying to an electron and a positron before annihilating to another photon.
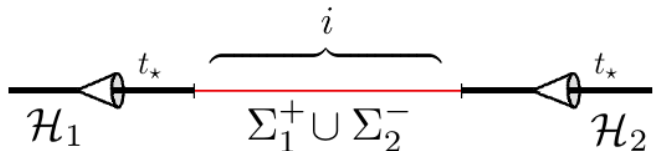

FIG. 7. This figure demonstrates the decomposition of $t_\star$ in $\mathcal{H}$ into its eigenspinor components during transit of the unit cell. This necessarily relies on a construction of complex numbers $z = x^0 + i\chi_\pm^5$ [9, 10] where the path over i is like an effective superposition of $t_\pm$ even when they are separated. Every string of time can have a representation as $t_\pm$ but the red i path might not be constructed from the $t_\pm$ of figure 6. $t_\star$ along i could equally well be constructed as the superposition of $t'_\pm$ comprising a circle perpendicular to the plane of the page.

time" with respect to which all other times evolve. When we consider figure 1 and there are only three time components, $t_\star$ does not contain more information than was in $t_\pm$. On the other hand, in a representation like figure 8, there will be free legs on the exterior of the circuit and everything between those legs and the $t_\star$ path of U will be defined such that $t_\star$ is maintained in a steady state on every other level of $\aleph$. We say every other level instead
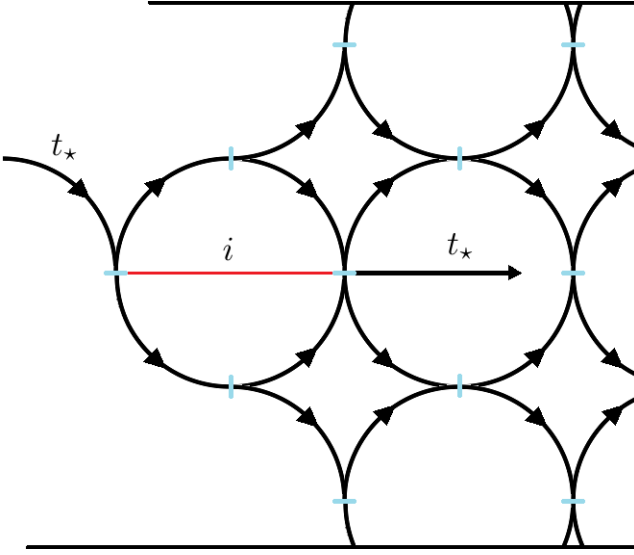
FIG. 8. This figure describes a general mechanism through which a trajectory of timelike evolution in Minkowski space $\mathcal{H}$ can enter the cosmological lattice. The foreground/background component on the right is evocative of the MCM idea to couple a gravitational background through dynamics rather than take QFT on an uncoupled spacetime background which does not properly gravitate. In the conformal coordinates of [10], the circles would be replaced with squares and the characteristics of convexity and concavity would be washed out. We expect that the precise connection between gravitation and electromagnetism should be inherited from the Kaluza–Klein theory [6, 19] which constrains 5D matter-energy in the bulk with a vanishing Ricci tensor. Gravitational waves satisfy $R_{AB} = 0$ so that will be a good channel through which a gravitational background can perturb a quantum state, and vice versa. In general, the qubit enters the lattice via the introduction of a quaternion phase whose commutation relations are those of the three Pauli matrices, up to a phase. Therefore, one is invited to consider three simultaneous levels of $\aleph$, each defined with a quaternion phase, as an advanced foreground, a middle whose observables are described with the Schrödinger operator ∂_t acting on states in Hilbert space, and a retarded background.

of every level because $|t_\star\rangle$ is an eigenspinor of $\hat{\sigma}^2$ only, not $\hat{\sigma}_i$. Superficially this seems to require two bounces in each unit cell but we might invoke some double counting for U and $\bar{U}$, or for a black/white hole pair in $\Sigma^\pm$. Later, we will give an even better reason for using two Pauli matrices.

Take special note of the operators $\hat{\sigma}_i^2$ which preserve a steady state of $t_\star$. In the case of angular momentum eigenspinors, the representation is an eigenspinor of $\hat{\sigma}_z$ *and also* the total angular momentum operator

$$\vec{\sigma}^2 \equiv \hat{\sigma}_1^2 + \hat{\sigma}_2^2 + \hat{\sigma}_3^2 \ . \tag{16}$$

Since our time arrow spinors are exactly the same as spin-1/2 angular momentum spinors, even when $t_\star$ is not an eigenspinor of $\hat{\sigma}_3$, it is an eigenspinor of $\hat{\sigma}_i^2$. This is written as

$$\hat{\sigma}_1^2|t_\star\rangle = |t_\star\rangle \tag{17}$$
$$\hat{\sigma}_2^2|t_\star\rangle = |t_\star\rangle \tag{18}$$
$$\hat{\sigma}_3^2|t_\star\rangle = |t_\star\rangle \ . \tag{19}$$

Any of these channels will preserve $|t_\star\rangle$ across the bounce but the $\hat{\sigma}_2^2$ channel is favored. Having demonstrated the eigenvalue relationships of both $\hat{\sigma}_3$ and $\hat{\sigma}_i^2$, and to some extent $\hat{\sigma}_1$ when $t_\pm$ have equal coefficients in $t_\star$, we see that the analogy between our time arrow spinors and the angular momentum system in quantum mechanics is quite robust. Therefore, we should also consider the ladder operators

$$\sigma^+ = \sigma_1 + i\sigma_2 = \begin{pmatrix} 0 & 2 \\ 0 & 0 \end{pmatrix} \ , \tag{20}$$

and

$$\sigma^- = \sigma_1 - i\sigma_2 = \begin{pmatrix} 0 & 0 \\ 2 & 0 \end{pmatrix} \ . \tag{21}$$

These operators give

$$\hat{\sigma}_+|t_+\rangle = 0 \tag{22}$$
$$\hat{\sigma}_-|t_+\rangle = 2|t_-\rangle \tag{23}$$
$$\hat{\sigma}_+|t_-\rangle = 2|t_+\rangle \tag{24}$$
$$\hat{\sigma}_-|t_-\rangle = 0 \ , \tag{25}$$

so for $t_\star$ we have

$$\hat{\sigma}_\pm|t_\star\rangle = 2c_\mp|t_\pm\rangle \tag{26}$$

What does this tell us? Superficially it looks useful for converting $t_\star$ to $t_\pm$ in the infinite complexity decomposition of the total time circuit. What about the concepts of raising and lowering? Can we use the raising and lowering operators to raise and lower the level of $\aleph$?

Writing the spin-up/down states in the more-complete $|j, m\rangle$ formalism we have

$$\left|\uparrow\right\rangle = \left|\frac{1}{2}, \frac{1}{2}\right\rangle \ , \qquad \text{and} \qquad \left|\downarrow\right\rangle = \left|\frac{1}{2}, -\frac{1}{2}\right\rangle \ . \tag{27}$$

Then

$$\hat{\sigma}_\pm\left|\frac{1}{2}, \mp\frac{1}{2}\right\rangle = 2\left|\frac{1}{2}, \pm\frac{1}{2}\right\rangle \tag{28}$$

We can use the m quantum number to put the level of $\aleph$ into the state as $\hat{\Phi}^{m+1/2}$ and ignore the j quantum number to write

$$\begin{aligned}
|t_\star\rangle &= c_+|t_+\rangle + c_-|t_-\rangle \\
&= c_+\left|\frac{1}{2}\right\rangle + c_-\left|-\frac{1}{2}\right\rangle \\
&= c_+|\hat{\Phi}^1\rangle + c_-|\hat{\Phi}^0\rangle \ .
\end{aligned} \qquad (29)$$

Since the m is unknown in the superposition state, that is like an observer in $\mathcal{H}$ being unable to determine his absolute level of $\aleph$ [10, 20]. In [2, 10], we made a strong argument that $t_\star$ is for even levels of $\aleph$ and that $t_\pm$ is for odd levels but equation (29) does not agree with the idea to put $t_\star$ on even levels of $\aleph$ and $t_\pm$ on odd levels. However, in [10], we made the case that the MCM might not always rely on adjacent levels of $\aleph$ and that sometimes it should use two objects on the same level. If we did want to preserve the interpretation that $t_\pm$ live on odd levels of $\aleph$, and not one odd and one even, as in equation (29), then the level of $\aleph$ should appear as $\hat{\Phi}^{2m}$ such that

$$|t_\star\rangle = c_+|\hat{\Phi}^1\rangle + c_-|\hat{\Phi}^{-1}\rangle \ , \qquad (30)$$

and

$$\hat{\sigma}_\pm|t_\star\rangle = 2c_\mp|\hat{\Phi}^{\pm 1}\rangle \ . \qquad (31)$$

In the above, we have neglected the plane wave part of the state. If we multiply our Pauli eigenspinors by $\psi = e^{ikx}$ then

$$|\psi;t_+\rangle = \begin{pmatrix} e^{ikx} \\ 0 \end{pmatrix} \ , \quad \text{and} \quad |\psi;t_-\rangle = \begin{pmatrix} 0 \\ e^{ikx} \end{pmatrix} \ . \qquad (32)$$

Furthermore, as in [10], we should replace the imaginary number i in ψ with a quaternion. This yields six spinors

$$\begin{array}{ll}
|\psi;t_+,\hat{\mathbf{i}}\rangle = \begin{pmatrix} e^{\mathbf{i}kx} \\ 0 \end{pmatrix} & |\psi;t_-,\hat{\mathbf{i}}\rangle = \begin{pmatrix} 0 \\ e^{\mathbf{i}kx} \end{pmatrix} \\[2ex]
|\psi;t_+,\hat{\mathbf{j}}\rangle = \begin{pmatrix} e^{\mathbf{j}kx} \\ 0 \end{pmatrix} & |\psi;t_-,\hat{\mathbf{j}}\rangle = \begin{pmatrix} 0 \\ e^{\mathbf{j}kx} \end{pmatrix} \quad (33) \\[2ex]
|\psi;t_+,\hat{\mathbf{k}}\rangle = \begin{pmatrix} e^{\mathbf{k}kx} \\ 0 \end{pmatrix} & |\psi;t_-,\hat{\mathbf{k}}\rangle = \begin{pmatrix} 0 \\ e^{\mathbf{k}kx} \end{pmatrix} \ ,
\end{array}$$

whose complexity exceeds that of the canonical Pauli spinors. Whatever kind of cosmological lattice site [11, 21] we use for $|t_\star\rangle$, meaning the label from among $\{\hat{i}, \hat{\Phi}, \hat{2}, \hat{\pi}\}$ attached to the $\hat{\sigma}_0$ leg of the bounce complex, these six spinors should represent the other three kinds of sites on two levels of $\aleph$. If one of those levels is the same as $t_\star$'s then we have four interacting sites on a single level, and a selection rule which says that one site has to go into another kind of site when it changes levels of $\aleph$. If the two levels of $\aleph$ encoded on the spinor are one higher and one lower then we maintain the selection rule: the $\hat{\sigma}_0$-site can't go to the $\hat{\sigma}_0$-site on an adjacent level

of $\aleph$. It would have to go to a $\hat{\sigma}_i$-site and it remains to be clarified how the Pauli-labeled sites should be labeled with $\{\hat{i}, \hat{\Phi}, \hat{2}, \hat{\pi}\}$. The second case in which neither of $t_\pm$ share a level of $\aleph$ with $t_\star$ might indicate that one kind of ontological site lives on even levels while the other three live on odd levels. We might even adjust the level of $\aleph$ in the dual vector of the bra-ket formulation so that a single site on the even level of $\aleph$ of $|t_\star\rangle$, call it the $\hat{\pi}$-site for example, would be complemented with the $\{\hat{2}, \hat{\Phi}, \hat{i}\}$-sites from $\langle t_\star|$ whose base level of $\aleph$ is odd. This latter option to put the bra on a higher level of $\aleph$ than the ket strongly agrees with the MCM bra-ket formalism developed in [22].

By including the quaternions in our definition of a plane wave, we add a new phase channel which should, in principle, add a lot to the spinor problem. For instance, where the classical bit is well-described with $|\Uparrow\rangle = 1$ and $|\Downarrow\rangle = 0$, the three orthogonal components of $e^{\mathbf{u}kx}$ are well-suited to describe a quantum bit having three states: 1, 0, and their superposition. For instance, one might write

$$\begin{aligned}
|\psi;t_+,\hat{\mathbf{i}}\rangle &= \begin{pmatrix} e^{\mathbf{i}kx} \\ 0 \end{pmatrix} \\
&= \begin{pmatrix} \cos(kx) + \mathbf{i}\sin(kx) \\ 0 \end{pmatrix} \\
&= \begin{pmatrix} \cos(kx) - i\hat{\sigma}_1\sin(kx) \\ 0 \end{pmatrix} \\
&= \begin{pmatrix} \cos(kx) & -i\sin(kx) \\ -i\sin(kx) & \cos(kx) \\ 0 & 0 \\ 0 & 0 \end{pmatrix} \ ,
\end{aligned} \qquad (34)$$

and then write three unique states as some combination of the spin-up and spin-down channel in each quaternion phase, possibly their tensor product yielding 4×4 matrices. Therefore, when the third state of a quantum bit is normally taken as a superposition which is linearly dependent on the other two, here we have the option to define three unique, independent matrices. This duality between two-fold and three-fold representations is mildly evocative of a supersymmetry between spin-$1/2$ and spin-1.

Note well: we can uniquely label the spinors as $\{\hat{i}, \hat{\Phi}, \hat{2}, \hat{\pi}\}$-sites in the MCM lattice hypercosmos [6]. $|t_\star\rangle$ is one kind of lattice site, call it $\hat{e}_0$ and the three quaternion phases on the eigenspinors are the other three kinds of lattice sites $\hat{e}_i$ on two distinct levels of $\aleph$. Above we considered the cases when the $m + 1/2$ quantum number dictates two adjacent levels of $\aleph$, and also when the $2m$ quantum number gives one higher level and one lower. We could also devise a scheme for two higher levels with another function of m. Whatever the technical nuance is, the algebra contains a selection rule that one kind of site can't transition to the same kind of site on the next level of $\aleph$, and that is quite similar to the Δl transition law in atomic physics. As we will want to increase the level of $\aleph$ by more than one or two in a realistic application, that

will require algorithmic renormalization which may be non-trivial in the quaternion phase. If we work in the most natural convention where the two distinct levels of $\aleph$ are those above and below that of $t_\star$ then we will have to implement the normalization procedure in every application of $\hat{M}^3$ because its output is two levels of $\aleph$ higher than its input.

STERN–GERLACH COSMOLOGY

The representation in figure 9 is evocative of the Stern–Gerlach experiment: one of the simplest experiments that demonstrate quantized spin. In the simplest variant of the experiment, an unpolarized beam of spin-1/2 silver atoms enter a region of inhomogeneous magnetic field. The energies of the spin-up and spin-down states are lowered via deflection in different directions through the magnetic field and then one is able to observe two separate splotches of silver on a plate at the end of the device. This is like the left side of figure 9. The so-called fancy Stern–Gerlach experiment adds more than one magnetic field. If it is exactly opposite to the first field then the beam will be recombined at the end of the device. Recombination can be derived from any arrangement of the fields when the integrated effect through the entire device is zero.

Now, we will demonstrate that the MCM unit cell is such that the analogue Stern–Gerlach apparatus is exactly the one which separates components and then recombines them so that the beam out is the same as the beam in. First, we need to show that the analogue field is inhomogeneous because the inhomogeneity of the $\vec{B}$ field is required for splitting in the lab experiment. The MCM Kaluza–Klein scalar field [6, 10, 19] is

$$\phi_\pm^2(\chi_\pm^5) = \chi_\pm^5 \quad , \tag{35}$$

so it does have the requisite inhomogeneity

$$\nabla\phi_\pm \neq 0 \quad , \tag{36}$$

built into it. This inhomogeneity would be preserved through a spin upgrade if we matched the spin of $\phi_\pm$ to that of $\vec{B}$. $\phi_\pm$ are oppositely signed in $\Sigma^\pm$ so the effect in one part of the bulk will be offset by the effect in the other part. To show that the effects in $\Sigma^\pm$ are exactly opposite such that the beam is perfectly recombined on $\mathcal{H}_2$, first consider that

$$\chi_-^5 \in [-1,0) \quad , \quad \text{and} \quad \chi_+^5 \in (0,\Phi] \quad , \tag{37}$$

would indicate unequal contributions from $\Sigma^\pm$. These are the $\chi_\pm^5$ around one instance of $\mathcal{H}$, corresponding to $\Sigma_1^\pm$. When crossing the unit cell from $\mathcal{H}_1$ to $\mathcal{H}_2$, we go

through χ_+^5 in Σ_1^+ and χ_-^5 in Σ_2^-, as in figure 2. Since Σ_2^- is on a higher level of $\aleph$, the size of the box has grown by Φ [10] giving

$$\chi_-^{5\,\{2\}} \in [-\Phi,0) \quad . \tag{38}$$

Therefore, we have everything needed to construct a cosmological Stern–Gerlach system inside the unit cell which will separate the $t_\pm$ components in the bulk and then recombine them on $\mathcal{H}_2$.

If χ_-^5 is to be reverse time with respect to χ_+^5, meaning that it decreases from $\aleph$ to $\mathcal{H}_2$, then

$$\chi_-^{5\,\{1\}} \in (0,1] \quad . \tag{39}$$

In that case, we will achieve $\chi_\pm^5 > 0$ in full analogy with the $y^\pm$ variables of hypercomplex $^\star\mathbb{C}$-numbers [9, 10]

$$z = x \pm iy_\pm \quad \longleftrightarrow \quad z = x^0 \pm i\chi_\pm^5 \quad . \tag{40}$$

When we make this change to the domain of χ_-^5, we can maintain all previous relationships by adding a minus sign where required, such as into the conformal coordinate $x^5 < 0$ which acts as the parameter of negative curvature in anti-de Sitter space [10]. Furthermore, the unit cell centered on $\varnothing$ may contain Σ^+ and Σ^- taken from U and $\bar{U}$ individually instead of both from a single universe. This mechanism of sampling from separate universes was suggested in [23] as a way to construct anti-symmetric spatial wavefunctions from symmetrical spaces. This contrasts the strict conception of figure 2 as the U_1 and U_2 legs of the bounce complex. Indeed, when $\Sigma^\pm$ are already on different levels of $\aleph$, it is natural to consider a unit cell constructed with

$$\Sigma_{\{1\}}^+ \cup \Sigma_{\{2\}}^- \quad \longleftrightarrow \quad \Sigma_{\{1\}}^+ \cup \bar{\Sigma}_{\{2\}}^- \quad . \tag{41}$$

This is very natural in the case where $t_\pm$ have equal coefficients in $t_\star$ because $|t_\star\rangle$ becomes an eigenspinor of the $\hat{\sigma}_1$ operator which sends U_1 into $\bar{U}_2$.
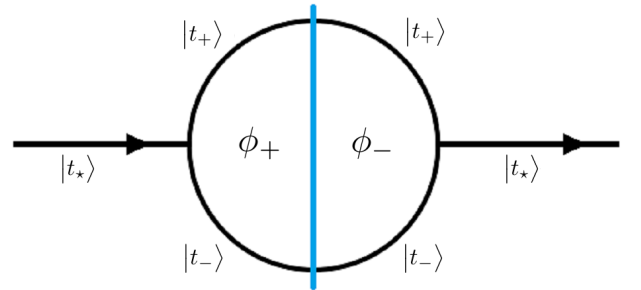

FIG. 9. This figure demonstrates a Stern–Gerlach cosmology in which the inhomogeneous $\vec{B}$ field is replaced with the Kaluza–Klein scalar field $\phi_\pm$. When the $\phi_\pm$ are oppositely signed in $\Sigma^\pm$, the Stern–Gerlach analogue effect separates $t_\pm$ and then recombines them.

Figure 10 demonstrates a few variants of the Stern–Gerlach experiment. On the first row, a beam is split into its spin-up and spin-down components, and the spin-down piece is sent into a beam dump. The spin-up polarized beam moves through another region of the same magnetic field and, as expected, the output beam contains no spin-down component. On the second row of figure 10, the polarized beam enters a region containing a different magnetic field, and the output beam contains spin-up and spin-down components written in the eigen-basis of $\hat{\sigma}_1$. This demonstrates that the z-directed $\vec{B}$ field labeled to the left with $\hat{\sigma}_3$ did not select for spin with respect to x. On the third row, the spin-down component with respect to x is sent to a beam dump and then the spin-up x-polarized beam enters a region containing the original magnetic field which separates again with respect to z. Even though the beam that enters the third magnetic field was already selected to have only spin-up states with respect to both x and z, the output beam contains spin-up and spin-down components with respect to z.

When we build the time circuit, this effect should be implemented such that correlations are washed out when they are separated by more than two levels of $\aleph$. In the cosmological analogue of figure 10's third row, we would consider $t_\star$ on $\hat{\Phi}^0$ as the leftmost beam source $\hat{\sigma}_0$. When $t_\star$ on even levels of $\aleph$ becomes $t_\pm$ on odd levels, the beam exiting the first $\hat{\sigma}_3$ apparatus is on $\hat{\Phi}^1$. Then the beam exiting the $\hat{\sigma}_1$ apparatus is like the part of the time circuit on $\hat{\Phi}^2$. Beyond the second $\hat{\sigma}_3$ apparatus, the logical coherence dissolves and that is well-suited to analogy in the hypercomplex analysis which considers at most three simultaneous levels of $\aleph$ [8, 10]. Considering the third row, note that the input beam is like $t_\star$ and the magnetic field separates it into $t_\pm$ components.
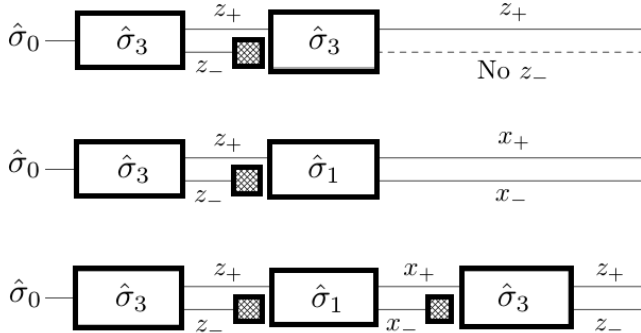

FIG. 10. This figure demonstrates the kernel of the quantum weirdness of the Stern–Gerlach experiment. On the bottom row, a beam which has been selected to only have spin-up components with respect to the z direction is observed to contain an anomalous spin-down component. The cosmological analogue should enforce the loss of correlations across levels of $\aleph$ separated by more than $\hat{\Phi}^2$. However, regarding loss of correlations, we should to examine whether or not the algebraic property of quaternions $\mathbf{ijk} = -1$ allows for a reverse passthrough channel through which information might be recovered.

Then we treat t_+ as $t'_\star$ and decompose that into its $t'_\pm$ components. Then we treat t'_+ as $t''_\star$, *etc.*

When one examines figure 10 and asks, "Why isn't $\hat{\Phi}^3$ correlated with $\hat{\Phi}^1$?," the answer should be that the polarization of the $\hat{\Phi}^1$ beam is impossible to know without filtering the $\hat{\Phi}^0$ beam. It is, therefore, impossible to consider $\hat{\Phi}^1$ in the absence of its correlation with $\hat{\Phi}^0$.

THE MCM HAMILTONIAN

The Stern–Gerlach experiment is described with the Pauli equation

$$i\frac{\partial}{\partial t}\left|\psi_\pm\right\rangle = \left\{\frac{1}{2m}\left[\vec{\sigma}\cdot\left(\hat{p}_x - q\vec{A}\right)\right]^2 + qA_0\right\}\left|\psi_\pm\right\rangle \ , \ (42)$$

where A_μ is an electromagnetic 4-vector potential, $\vec{A}\equiv A_i$, and $\psi_\pm$ is a two-component spinor. This is the simplest extension of the Schrödinger equation to include spin-1/2. The Stern–Gerlach interaction is isolated from the Schrödinger part as

$$\hat{H}_{\text{SG}} = -\frac{q}{2m}\,\vec{\sigma}\cdot\vec{B} \ . \qquad (43)$$

This follows from identity

$$\left(\vec{\sigma}\cdot\vec{F}\right)^2 = \vec{F}^2 + i\vec{\sigma}\cdot\left(\vec{F}\times\vec{F}\right) \ , \qquad (44)$$

where $\vec{F}\times\vec{F}$ doesn't identically vanish due to the operator properties of $\vec{p}=-i\vec{\nabla}$ in $\vec{F}=\vec{p}-q\vec{A}$.

We have time arrow states $|t_\pm\rangle$, not spin states $|\psi_\pm\rangle$, so what should be the cosmological analogue of equations (42) and (43)? We need to closely examine the ∂_t operator, the charge q, the mass m, and the field $\vec{B}$ to determine their cosmological analogues. First consider the Schrödinger equation's derivative with respect to t. This t is like the "emergent" time described above because everything else in the quantum theory evolves according to it but it is not emergent; it is purely external. In the Schrödinger (Pauli) equation, t is strictly x^0. We may separate the Schrödinger operator ∂_t from the $t_\pm$ components with a definition that $\chi^5_\varnothing$ is the random superposition of $\chi^5_\pm$ while x^0 is the special top-level time with respect to which all other things evolve, or vice versa. For instance, if we choose $\chi^5_\varnothing\equiv t_\star$ then $t_\star$ is unlike the $t\equiv x^0$ in the Schrödinger operator ∂_t. When we choose one of $\{x^0, \chi^5_\varnothing\}$ for one purpose, the other is left for the other. This construction is ready-made for experimental applications whose formalism doesn't allow us to mess with $x^0\equiv t$. Therefore, we should replace ∂_t with cases for ∂_0 and ∂_5.

The charge q in the Stern–Gerlach Hamiltonian should be replaced with p^0. The energy p^0 is oppositely signed

in U and $\bar{U}$ as required to achieve two opposite deflection directions within the bulk of the MCM unit cell. In the quantum theory, p^0 will be an operator and its returned value will be oppositely signed when it operates on $|t_\pm\rangle$. When $\hat{p}^0 \to -i\partial_0$ is the timelike part of the 4-momentum, we can separate this piece from the time derivative ∂_t which is built into the Schrödinger equation by relabeling it p^5 corresponding to $\chi_\pm^5$. We might also leave it as p^0 and replace x^0 in the time derivative with $\chi_\varnothing^5$. We want to make sure that p^0 becomes something not identical to the ∂_t Schrödinger operator. As we have the freedom to study general relativity as the propagation of a spacelike 3-space along either of $\{x^0, \chi_\pm^5, \chi_\varnothing^5\}$, so too do we have the freedom to evolve a quantum state with a Schrödinger equation whose derivative ∂_t is with respect to any of $\{x^0, \chi_\pm^5, \chi_\varnothing^5\}$.

The cosmological analogue of $\vec{B}$ should be like the Kaluza–Klein scalar field $\phi_\pm$, as in figure 9. Where $\vec{B}$ is a spin-1 field, we might upgrade $\phi_\pm$ to spin-1 via the inclusion of polarization quaternions $\{\mathbf{i}, \mathbf{j}, \mathbf{k}\}$. The cosmological Stern–Gerlach analogue Hamiltonian can be fully specified with quaternions because the Pauli matrices are isomorphic to the quaternions with

$$\mathbf{i}^2 = \mathbf{j}^2 = \mathbf{k}^2 = -1 \qquad \longleftrightarrow \qquad \hat{\sigma}_i^2 = \hat{\sigma}_0 \quad , \qquad (45)$$

and

$$\mathbf{ijk} = -1 \qquad \longleftrightarrow \qquad \hat{\sigma}_1 \hat{\sigma}_2 \hat{\sigma}_3 = i\hat{\sigma}_0 \quad , \qquad (46)$$

altogether implying that

$$\hat{\mathbf{u}}_i \quad \longleftrightarrow \quad -i\hat{\sigma}_i \quad , \qquad \text{and} \qquad \hat{1} \quad \longleftrightarrow \quad \mathbb{I} \quad , \quad (47)$$

with $\hat{\mathbf{u}}_i \in \{\mathbf{i}, \mathbf{j}, \mathbf{k}\}$. When we implement the intermediate renormalization which allows us to go to a second higher level of $\aleph$ while the spinor algebra gives one higher level and one lower, we would be well-motivated to consider a relationship

$$\hat{\mathbf{q}}_\mu \quad \longleftrightarrow \quad -i\hat{\sigma}_\mu \quad , \qquad (48)$$

that carries the imaginary part into the Pauli identity via $\hat{\mathbf{q}}_\mu \in \{\hat{1}, \mathbf{i}, \mathbf{j}, \mathbf{k}\}$. Indeed, note that

$$(\mathbf{ijk})^2 \mathbb{I} = \mathbb{I} \quad , \qquad \text{and} \qquad (\hat{\sigma}_1 \hat{\sigma}_2 \hat{\sigma}_3)^2 = -\mathbb{I} \quad , \quad (49)$$

gives a natural channel for an extra layer of phase. We will revisit these *complex* phase issues in the quaternion-dedicated section.

Regarding the cosmological analogue of $\hat{H}_{\text{SG}}$, let

$$\vec{\sigma} \to i\hat{\mathbf{u}}_1 \quad , \qquad \text{and} \qquad \vec{B} \to i\phi_\pm \hat{\mathbf{u}}_2 \quad , \qquad (50)$$

so that we arrive at

$$\hat{H}_{\text{MCM}}^{\Sigma^\pm} = \frac{\hat{p}^0}{2m} \, \hat{\mathbf{u}}_1 \phi_\pm \hat{\mathbf{u}}_2 \quad . \qquad (51)$$

We have included the i in the $\vec{B}$ part of definitions (50) to keep the energy real and we could add a minus sign as needed. Noting that $p^0 = E$ and that the non-relativistic energy of our non-relativistic Pauli spinors is $E = m$ in units where $c^2 = 1$, we may simplify the MCM Hamiltonian as

$$E_{\text{MCM}}^{\Sigma^\pm} = \frac{1}{2} \big| \hat{\mathbf{u}}_1 \phi_\pm \hat{\mathbf{u}}_2 \big| \quad . \qquad (52)$$

E_{MCM} is minimized in $\mathcal{H}$ at $\chi_\pm^5 = 0$ through the definition $\phi_\pm^2 = \chi_\pm^5$ [10, 16, 19, 24]. Note the agreement with the MCM description of the maximum action path [6, 11, 25] as the one which pulls a trajectory out of $\mathcal{H}_1$ and across hyperspacetime until it falls into another minimum in $\mathcal{H}_2$ on a higher level of $\aleph$ (where $\chi_\pm^{5\,\{2\}} = 0$.) In equations (51) and (52), we use the notation that an arbitrary, unhatted, non-unit quaternion is

$$\mathbf{q} = u_0 \hat{1} + \mathbf{u} \quad , \qquad \text{with} \qquad \mathbf{u} = c_i \mathbf{i} + c_j \mathbf{j} + c_k \mathbf{k} \quad , \quad (53)$$

while $\{\mathbf{i}, \mathbf{j}, \mathbf{k}\}$ are identically unit quaternions. We only put the unit quaternion $\hat{\mathbf{u}}$ into $\hat{H}_{\text{MCM}}$ and not the more general $\hat{\mathbf{q}}$ because $\hat{1}$ is reserved for the Schrödinger part of the total Hamiltonian in the Pauli equation. This is demonstrated in

$$i\frac{\partial}{\partial t}|\psi_\pm\rangle = \left\{ \left[\frac{(\hat{p}_x - q\vec{A})^2}{2m} + qA_0 \right] \hat{1} - \frac{q}{2m}\vec{B} \cdot \vec{\sigma} \right\} |\psi_\pm\rangle \quad . \qquad (54)$$

When developing the rudiments of the time circuit in figure 5, we found that we needed to use two Pauli matrices to preserve $|t_\star\rangle$. Now we see that two quaternions appear in the Stern–Gerlach analogue Hamiltonian, equation (52). The specific condition for preserving $|t_\star\rangle$ (with unequal coefficients for $t_\pm$) was that the two Pauli matrices must be the same, *i.e.*: $|t_\star\rangle$ is an eigenspinor of $\hat{\sigma}_i^2$ but not $\hat{\sigma}_j \hat{\sigma}_k$ for $j \neq k$. When we use the isomorphism with the quaternion representation and set $\hat{\mathbf{u}}_1 = \hat{\mathbf{u}}_2$ in equation (52), we get a very familiar looking energy function. When $\hat{\mathbf{u}}$ is a 3-velocity in the bulk of the MCM unit cell and the scalar field $\phi_\pm$ is a mass analogue, equation (52) becomes identically the kinetic energy. Indeed, when the $\hat{\mathbf{u}}$ are two unit quaternions, their product is very much like the spatial 4-velocity which is normalized such that

$$U^\mu U^\mu g_{\mu\nu} = -1 \quad . \qquad (55)$$

If we replace the 3-velocity $\vec{v}$ in U^μ with $\hat{\mathbf{u}}$ then time stops for $\hat{\mathbf{u}}_1 \hat{\mathbf{u}}_2 = -1$ which is the property of any two like unit quaternions $\{\mathbf{i}, \mathbf{j}, \mathbf{k}\}$.

Equation (51) preserves the spin-0 character of the Kaluza-Klein field. If we promote $\phi_\pm$ to spin-1 then we would write

$$\vec{B} \quad \longrightarrow \quad i\boldsymbol{\phi}_\pm = i\phi_{\mathbf{i}\pm}\mathbf{i} + i\phi_{\mathbf{j}\pm}\mathbf{j} + i\phi_{\mathbf{k}\pm}\mathbf{k} \quad . \tag{56}$$

In definitions (50), we multiplied a unit quaternion $\hat{\mathbf{u}}$ by a scalar $\phi_\pm$ and now we consider a non-unit quaternion $\boldsymbol{\phi}_\pm$. Taking $\boldsymbol{\phi}_\pm$ and the long form of $\hat{\mathbf{u}}_1$ from equations (53), plugging them into equation (52) yields

$$\hat{H}_{\mathrm{MCM}}^{\Sigma\pm} = \frac{\hat{p}^0}{2m}\left(\hat{\mathbf{u}}_1 \times \boldsymbol{\phi}_\pm - \sum_{n=1}^{3} c_n \phi_{n\pm}\right) \quad . \tag{57}$$

This follows from the property of quaternions

$$\begin{array}{lll} \mathbf{ij} = \mathbf{k} & \mathbf{jk} = \mathbf{i} & \mathbf{ki} = \mathbf{j} \\ \mathbf{ji} = -\mathbf{k} & \mathbf{kj} = -\mathbf{i} & \mathbf{ik} = -\mathbf{j} \end{array} \quad , \tag{58}$$

which translates to the Pauli matrices as

$$\begin{array}{lll} \hat{\sigma}_1\hat{\sigma}_2 = i\hat{\sigma}_3 & \hat{\sigma}_2\hat{\sigma}_3 = i\hat{\sigma}_1 & \hat{\sigma}_3\hat{\sigma}_1 = i\hat{\sigma}_2 \\ \hat{\sigma}_2\hat{\sigma}_1 = -i\hat{\sigma}_3 & \hat{\sigma}_3\hat{\sigma}_2 = -i\hat{\sigma}_1 & \hat{\sigma}_1\hat{\sigma}_3 = -i\hat{\sigma}_2 \end{array} \quad . \tag{59}$$

In the Stern–Gerlach part of equation (54), there will be at most three terms derived from $\vec{\sigma} \cdot \vec{B}$: $\hat{\sigma}_1 B_x$, $\hat{\sigma}_2 B_y$, and $\hat{\sigma}_3 B_z$. In the cosmological analogue, equation (57), there is a fourth term in $\hat{\mathbf{u}}_1\hat{\mathbf{u}}_2$. Since we are not considering an electromagnetic field at all in the cosmological analogue, this fourth term should replace the qA_0 term in the Schrödinger part of equation (54).

The spin-1 formulation is not inherent to the Kaluza–Klein field on which the MCM is constructed [19], and the spin-1 formulation disrupts the eloquence of the kinetic energy formulation, equation (52), even while it is essentially equivalent. Therefore, consider the changes to the Stern–Gerlach Hamiltonian

$$\vec{\sigma} \to i\hat{\mathbf{u}}_1\hat{\mathbf{u}}_2 \quad , \quad \text{and} \quad \vec{B} \to i\boldsymbol{\phi}_\pm \quad , \tag{60}$$

such that $\phi_\pm$ remains scalar. This formulation which upgrades the single Pauli matrix to a pair of quaternions demonstrates the cosmological complexification of the Stern–Gerlach Hamiltonian. The vector product of $\vec{\sigma}$ and $\vec{B}$ gives at most three terms but the product of two quaternions gives up to four terms. The total cosmological Hamiltonian is

$$\hat{H}_{MCM}^{\Sigma\pm} = \frac{\hat{p}_x^2}{2m} + \frac{\hat{p}^0}{2m}\,\hat{\mathbf{u}}_1\hat{\mathbf{u}}_2\phi_\pm \quad , \tag{61}$$

and the $\pm$ cases refer to the energies in $\Sigma^\pm$ respectively. When we multiply out the quaternion product we get

$$\hat{H}_{MCM}^{\Sigma\pm} = \frac{\hat{p}_x^2}{2m} + \frac{\hat{p}^0}{2m}\,\phi_\pm\big(\hat{\mathbf{u}}_1 \cdot \hat{\mathbf{u}}_2 + \hat{\mathbf{u}}_1 \times \hat{\mathbf{u}}_2\big) \quad . \tag{62}$$

We extend the vector dot and cross products to quaternions as

$$\hat{\mathbf{u}}_1\hat{\mathbf{u}}_2 = \hat{\mathbf{u}}_1 \cdot \hat{\mathbf{u}}_2 + \hat{\mathbf{u}}_1 \times \hat{\mathbf{u}}_2 \tag{63}$$

$$\hat{\mathbf{u}}_1 \cdot \hat{\mathbf{u}}_2 = -\sum_{n=1}^{3} c_{1_n} c_{2_n} \tag{64}$$

$$\begin{aligned} \hat{\mathbf{u}}_1 \times \hat{\mathbf{u}}_2 = \mathbf{u}_3 = &\,\hat{\mathbf{i}}\left(c_{1_2}c_{2_3} - c_{1_3}c_{2_2}\right) + ... \\ &... + \hat{\mathbf{j}}\left(c_{1_3}c_{2_1} - c_{1_1}c_{2_3}\right) + ... \\ &... + \hat{\mathbf{k}}\left(c_{1_1}c_{2_2} - c_{1_2}c_{2_1}\right) \quad , \end{aligned} \tag{65}$$

and we will condense terms as

$$\hat{\mathbf{u}}_1 \cdot \hat{\mathbf{u}}_2 = -Z \quad , \quad \text{and} \quad \mathbf{u}_3 \equiv -i\vec{\sigma} \quad , \tag{66}$$

where $\vec{\sigma}$ is a non-unit Pauli matrix.

To crunch the Pauli equation with $\hat{H}_{MCM}^{\Sigma\pm}$, consider only Σ^+ to avoid ambiguity with the $\pm$ specifying the $\psi_\pm \to t_\pm$ spinor (which contributes to the sign of p^0). The Hamiltonian is

$$\hat{H}_{MCM}^{\Sigma+} = \frac{\hat{p}_x^2 - \hat{p}^0\phi_+\big(Z + i\vec{\sigma}\big)}{2m} \quad . \tag{67}$$

It follows from equations (63) and (66) that

$$Z = 1 \quad \implies \quad \vec{\sigma} = 0 \tag{68}$$

and

$$\vec{\sigma} = \hat{\sigma}_3 \quad \implies \quad Z = 0 \quad , \tag{69}$$

so we will consider these simplifying cases when we derive the dispersion relations of the modes allowed by the MCM Hamiltonian. Furthermore, we consider only $|t_+\rangle$. We can put the pieces all together as

$$i\frac{\partial}{\partial\chi_{\varnothing}^5}\,|t_+\rangle = \left(\frac{\hat{p}_x^2 - \hat{p}^0\phi_+\big(Z + i\vec{\sigma}\big)}{2m}\right)\Big|t_+\Big\rangle \quad . \tag{70}$$

We have changed the Pauli equation's ∂_t to ∂_5 to illustrate propagation across the unit cell but we could equally well leave it as ∂_t and rewrite p^0 as p^5 such that

$$i\frac{\partial}{\partial x^0}\,|t_+\rangle = \left(\frac{\hat{p}_x^2 - \hat{p}^5\phi_+\big(Z + i\vec{\sigma}\big)}{2m}\right)\Big|t_+\Big\rangle \quad . \tag{71}$$

These two equations should describe chirological and chronological evolution respectively. We will derive the allowed frequencies and label them $\omega_\chi(Z)$ and $\omega_x(Z)$.

The spinor is

$$|t_+\rangle = \begin{pmatrix} \psi \\ 0 \end{pmatrix} \quad , \tag{72}$$

and ψ needs to depend on χ^5 if equation (70) is to be non-trivial. We will make a definition that

$$\frac{\partial}{\partial \chi_\varnothing^5} \chi_\pm^5 \equiv \partial_5 \chi_\pm^5 = \pm 1 \quad , \tag{73}$$

and select a wavefunction

$$\psi = e^{-i(\omega t - kx \pm \chi_\pm^5)} \quad , \tag{74}$$

which is very natural because $\chi_\pm^5 = 0$ in $\mathcal{H}$. A more complete treatment would look at

$$\psi' = e^{-\mathbf{u}(\omega t - kx \pm \chi_\pm^5)} \quad , \tag{75}$$

and this formulation would necessarily require a revision to the i attached to the Schrödinger operator ∂_t.

The chirological Pauli equation gives

$$i\frac{\partial}{\partial \chi_\varnothing^5} |t_+\rangle = \left(\frac{-\partial_x^2 + i\partial_0 \phi_+ \left(Z + i\vec{\sigma} \right)}{2m} \right) |t_+\rangle \tag{76}$$

$$|t_+\rangle = \left(\frac{k^2 + \omega \phi_+ \left(Z + i\vec{\sigma} \right)}{2m} \right) |t_+\rangle \quad . \tag{77}$$

In the limiting cases of $\hat{\mathbf{u}}_1$ and $\hat{\mathbf{u}}_2$ parallel or perpendicular we obtain

$$\omega_\chi(1) = \frac{2m - k^2}{\phi_+} \tag{78}$$

$$\omega_\chi(0) = i\frac{k^2 - 2m}{\phi_+} \quad . \tag{79}$$

Neither of these look like the classical limit $\omega = k^2/2m$ (which follows from $E = \hbar\omega$ and $p = \hbar k$ in units where $\hbar = 1$.) The chronological Pauli equation, the one in which we definitely should find the classical limit, is

$$i\frac{\partial}{\partial x^0} |t_+\rangle = \left(\frac{-\partial_x^2 + i\partial_5 \phi_+ \left(Z + i\vec{\sigma} \right)}{2m} \right) |t_+\rangle \tag{80}$$

$$\omega |t_+\rangle = \left(\frac{k^2 + \phi_+ \left(Z + i\vec{\sigma} \right)}{2m} \right) |t_+\rangle \quad . \tag{81}$$

This gives

$$\omega_x(1) = \frac{k^2 + \phi_+}{2m} \tag{82}$$

$$\omega_x(0) = \frac{k^2 + i\phi_+}{2m} \quad , \tag{83}$$

which obviously does contain the classical energy where $\phi_+ = 0$. Since $\phi_\pm^2(\chi_\pm^5) = \chi_\pm^5$, $\phi_+ = 0$ in $\mathcal{H}$ and we see that the Hamiltonian is completely robust. One notices that we could use $\phi_\pm^2$ as the cosmological analogue for $\vec{B}$ instead of the linear incarnation $\phi_\pm$. In that case, there would be some subtlety related to the definition of the scalar field as

$$\phi_\pm^2(\chi_\pm^5) = \chi_\pm^5 \quad , \qquad \text{or} \qquad \phi_\pm^2 \equiv \chi_\pm^5 \quad . \tag{84}$$

In the former case, ∂_5 will not operate on ϕ_+^2 and we obtain

$$\omega_x(1) = \frac{k^2 + \phi_+^2}{2m} \tag{85}$$

$$\omega_x(0) = \frac{k^2 + i\phi_+^2}{2m} \quad . \tag{86}$$

However, when $\phi_\pm^2 \equiv \chi_\pm^5$ we get

$$i\frac{\partial}{\partial x^0} |t_+\rangle = \left(\frac{-\partial_x^2 + i\partial_5 \chi_+^5 \left(Z + i\vec{\sigma} \right)}{2m} \right) |t_+\rangle \tag{87}$$

$$\omega |t_+\rangle = \left(\frac{k^2 + i \left(Z + i\vec{\sigma} \right)}{2m} \right) |t_+\rangle \quad , \tag{88}$$

which gives

$$\omega_x(1) = \frac{k^2 + i}{2m} \tag{89}$$

$$\omega_x(0) = \frac{k^2 - 1}{2m} \quad . \tag{90}$$

This formulation does not seem particularly interesting so we should assume that ∂_5 does not operate on $\phi_\pm$.

These energies exhibit interest behavior in the limits where the two unit quaternions in $\hat{H}_{\mathrm{MCM}}^{\Sigma^+}$ are parallel with $Z = 1$ or perpendicular with $\vec{\sigma} = \hat{\sigma}^3$. For $\omega_\chi(Z)$, the two cases give a totally real or totally imaginary frequency. An imaginary frequency is likely associated with propagation across the unit cell rather than within a single universe. For $\omega_x(Z)$, the classical limit exists in both cases and it is modified with a real or imaginary component. Namely, the totally real classical frequency stays real and increases with ϕ_+ when $\hat{\mathbf{u}}_1$ and $\hat{\mathbf{u}}_2$ are parallel but the frequency becomes complex when they are perpendicular. Therefore, the $Z = 0$ case of $\hat{\mathbf{u}}_1$ perpendicular to $\hat{\mathbf{u}}_2$ is a special case for the Hamiltonian in the chirological evolution equation which uses ∂_5 as the Schrödinger operator. What does it mean if the two unit quaternions are parallel or perpendicular? In the next section, we will show how these can be lattice vectors in a fractal hypercosmological lattice such that bispinor structure allows for a Hopf fibration time circuit template whose nodes should be constrained to have internal multiplectic structure which is also a Hopf fibration.

HOPF FIBRATION TIME CIRCUIT TEMPLATE

When one asks, "How can I put this on a computer?," a likely template is the $\mathbb{R}^3$ boundary condition defined by the Hopf fibration. Most boundary conditions in $\mathbb{R}^3$ are available as software modules, and softwares for modeling in 3D are well-known. In the original MCM construction of the time circuit [1], we arranged the lattice so that $\{t_+, t_\star, t_-\}$ were parallels, meridians, and hypermeridians on the surface of a 3-sphere, as in figure 11. These three types of circles, having infinite radii in their incarnations as straight lines, meet at orthogonal triads such that the cross product of any two different tangent vectors at the point of intersection gives a tangent vector pointing along the third direction [1]. This is entirely consistent with our intention to use the quaternions as analogue velocities because a velocity is, by construction, the tangent vector to some curve. Therefore, when we take $\hat{\mathbf{u}}_1$ and $\hat{\mathbf{u}}_2$ as the tangent vectors to parallels, meridians, and hypermeridians meeting at cosmological lattice sites, they will always be parallel or perpendicular giving the cases of $Z \in \{1, 0\}$ considered above for the MCM Hamiltonian because those three elements always meet at right orthogonal vertices. Then, in the usual way, the symmetries of the system can be represented with energy functions of its lattice vectors [10, 26].

The Hopf fibration, which is visualized through its stereographic projection into $\mathbb{R}^3$ as parallels, meridians, and hypermeridians, is constructed by "fibrating" a circle from every point in $\mathbb{S}^2$. $\mathbb{S}^2$ is the topology of the boundary of the dynamical 3-space, the closed or open 3D spatial part of dS, AdS, or Minkowski space, whose quantum states are described with quantum mechanics so the Hopf fibration is a natural construction on which to consider a time circuit that can shift everything out of spacetime, into hyperspacetime, along the added degree of freedom afforded by the fibration. Indeed, we described the overall process of $\hat{M}^3$ as a periodic orbit of the Hopf fibration [17, 23, 27].

To understand a little about the physics of the Hopf template for the time circuit, we need to examine what a unit velocity is because usually velocities range over a spectrum. Earlier we remarked that the unit velocity condition is quite like the normalization of the 4-velocity

$$U^\mu U^\mu g_{\mu\nu} = -c^2 \quad . \tag{91}$$

When the observer is at rest, meaning the 3-velocity $\vec{v} = 0$, the observer has unit 1-velocity in units where $c = 1$. The 1-velocity is the rate of passage of time as opposed to the rate of passage of length described by the 3-velocity. The fundamental principle of relativity is that the 1-velocity is always constant in the observer's inertial frame. If, somehow, a physical observer had $|\vec{v}| = c$, which is a unit velocity in units where $c = 1$, then time would stop but relativity requires that an infinite amount of kinetic energy is required to get a massive object all the way up to $v = 1$. This is also the reason why photons don't experience time and it seems like there is some interesting connection between the three polarizations of
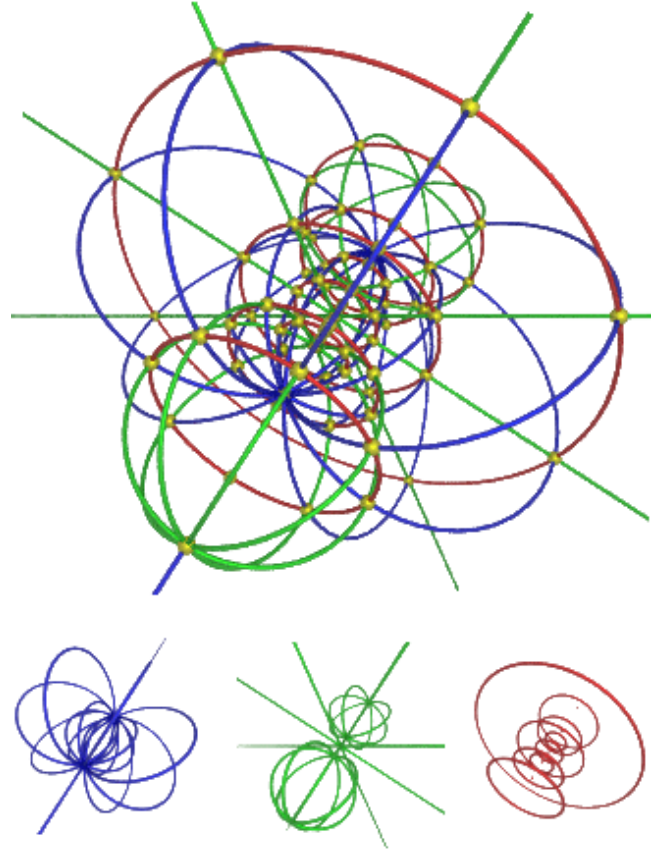

FIG. 11. This figure shows the projection of the Hopf fibration into $\mathbb{R}^3$. We should use this structure as a template for the time circuit wherein the quaternion phase indicates whether a particular plane wave propagates along the circuit's parallels, meridians, or hypermeridians. From left to right across the bottom are blue meridians, green hypermeridians, and red parallels, and there exist independent channels for a "second quantized" imaginary quaternion phase within each quaternion phase.

the spin-1 photon and the three quaternion phases, and also between the on-shell condition which eliminates one polarization for the massless photon, and the dual condition that $t_\star$ depends on $t_\pm$. So, how shall we obtain unit velocity? By moving along $\chi^5_\pm$, horizontally across the unit cell, that sets automatically the 1-velocity to zero via propagation along $\chi^5_\pm$ orthogonal to x^0. Therefore, we obtain unit relativistic 3-velocities along that path via the normalization of the 4-velocity. We have shown that propagation along $\chi^5_\pm$ from $\mathcal{H}_1$ to $\mathcal{H}_2$ must be faster than light [26] so we are compelled to consider non-unit quaternions which would denormalize the 4-velocity. We will develop those non-unit quaternions now and then show how they should be objects in the Hopf circuit.

In [22], we developed the matrix element of $\hat{M}^3$ as the quaternion rotation of a ordinary rotation operator. The unitary evolution operator that is constructed from the quantum mechanical Hamiltonian is one such ordinary rotation operator so we deemed to add complexity to the formalism of quantum mechanics with

$$\langle\psi|e^{i\hat{H}t}|\psi\rangle \quad \longrightarrow \quad \langle\psi|e^{-\hat{\mathbf{u}}_2\theta}e^{i\hat{H}t}e^{\hat{\mathbf{u}}_1\theta}|\psi\rangle \ . \tag{92}$$

This gives the MCM formalism which specifies the lattice site through

$$\langle\psi|e^{-\hat{\mathbf{u}}_2\theta}e^{i\hat{H}t}e^{\hat{\mathbf{u}}_1\theta}|\psi\rangle = \langle\psi;-\hat{\mathbf{u}}_2\theta|e^{i\hat{H}t}|\psi;\hat{\mathbf{u}}_1\theta\rangle \ , \tag{93}$$

where $\theta \in \{i,\Phi,2,\pi\}$ [21, 26]. For instance, we might define some lattice symmetry with non-unit quaternions $\hat{\mathbf{u}}\Phi \equiv \boldsymbol{\Phi}$. In this way, we can write the $\Phi\pi$ matrix element of $\hat{M}^3$ as

$$\langle\psi|\hat{M}^3_{\Phi\pi}|\psi\rangle = \langle\psi;\boldsymbol{\Phi}|e^{i\hat{H}t}|\psi;\boldsymbol{\pi}\rangle \ . \tag{94}$$

Therefore, where a quaternion rotation is strictly defined by $\hat{\mathbf{u}}_1^{-1}\hat{\mathbf{u}}_1$, we can make an analogue pseudo-quaternion rotation of two unequal quaternions $\hat{\mathbf{u}}_2^{-1}\hat{\mathbf{u}}_1$ by operating to the left and right in the bra-ket and then taking the inner product. Whatever the resultant phase is, that defines the asymmetric pseudo-quaternion rotation. Indeed, an octonion is comprised of two independent quaternions but we want one real quaternion and one imaginary, as detailed in a following section.

We have shown [21] that the dyadic tensor product of the ontological basis $\{\hat{i},\hat{\Phi},\hat{2},\hat{\pi}\}$ with itself has sixteen matrix elements, as does the Clifford algebra of the Dirac equation. Likewise, equation (94) shows one of sixteen matrix elements of $\hat{M}^3$. We are, therefore, invited to consider cosmological lattice sites labeled with pairs from the ontological basis instead of singles, so that there are sixteen types of sites instead of only four. The non-relativistic bispinor formulation of the MCM spinors is

$$|\psi;t_+,\mathbf{i}\rangle = \begin{pmatrix} \cos(kx) & -i\sin(kx) \\ -i\sin(kx) & \cos(kx) \\ 0 & 0 \\ 0 & 0 \end{pmatrix} \ , \tag{95}$$

where, for example,

$$|\psi;t_\star;\boldsymbol{\Phi}\rangle \equiv \Phi|\psi;t_+,\mathbf{i}\rangle \otimes |\psi;t_-,\mathbf{i}\rangle \ , \tag{96}$$

so that

$$|\psi;t_\star;\boldsymbol{\Phi}\rangle = \begin{pmatrix} \Phi\mathcal{C} & -i\Phi\mathcal{S} & 0 & 0 \\ -i\Phi\mathcal{S} & \Phi\mathcal{C} & 0 & 0 \\ 0 & 0 & \mathcal{C} & -i\mathcal{S} \\ 0 & 0 & -i\mathcal{S} & \mathcal{C} \end{pmatrix} \ , \tag{97}$$

where $\mathcal{C}=\cos(kx)$ and $\mathcal{S}=\sin(kx)$. Therefore, when we consider the relativistic limit in which the chronological space without identical topological flatness begins to exhibit its mode of curvature, our MCM spinors and operators are well-suited to matrix multiplication operations with the elements of the bispinor Dirac theory. In the

non-relativistic limit of the Dirac equation, the bottom two spinor components go to zero, but we have two or four columns in our multiplectic state because we have inflated the spinor with a quaternion instead of a second spinor. When we add the quaternion phase to the bispinor state of relativistic quantum mechanics, a.k.a the quantum field theory of light and matter, in extension of what we have shown here for the non-relativistic state, it is likely that the matrix objects will become non-trivially more complicated. Indeed, if we onvoke the octonions then it will become true that certain of the algebraic properties cannot be represented with matrices. However, if we the spectrum of our non-unit quaternions does not generate and identical octonion then, by virtue of the linearity of quantum mechanics, everything will remain within the ordinary bounds of matrix algebra.

Now we have three types of plane wave states, and we want each one to propagate along a different sub-circuit of the the time circuit such that they interact at nodes. The sub-circuits are the parallels, meridians, and hyper-meridians, and, when we construct states $|\psi;\{\mathbf{2},\boldsymbol{\Phi},\boldsymbol{\pi}\}\rangle$, we might use the labels on ψ to specify a particular sub-circuit. First we will consider a node within a single sub-circuit, that associated with $\mathbf{i}$, such that the unit quaternion velocities $\hat{\mathbf{u}}_1$ and $\hat{\mathbf{u}}_2$ are parallel but pointing in opposite directions. This leads to

$$-\mathbf{ii} = 1 \ . \tag{98}$$

The quaternion phase is totally scrubbed. Now consider a node at the intersection of two sub-circuits such that

$$\mathbf{ij} = \mathbf{k} \ . \tag{99}$$

This tells us that the two plane waves which entered the node along their respective sub-circuits will exit the node along the third sub-circuit. Finally, when components from all three sub-circuits meet at a node we get

$$\mathbf{ijk} = 1 \ . \tag{100}$$

Now further consider that the interaction with the node is described with the inner product. Along a single sub-circuit we get

$$\langle\psi;-\mathbf{i}|\psi;\mathbf{i}\rangle = 1 \ , \tag{101}$$

but at the intersection of two sub-circuits we get

$$\langle\psi;\mathbf{j}|\psi;\mathbf{i}\rangle = -\mathbf{k} \ . \tag{102}$$

For the probability interpretation, these numbers need to be in $\mathbb{R}$ but $\mathbf{k}\notin\mathbb{R}$. This is evocative of an issue raised in [22], namely regarding the difference between discrete and continuous state spectra. For discrete states, we have

$$\langle \psi_n | \psi \rangle = \alpha_n \quad , \tag{103}$$

and

$$P[\psi_n] = \sum_{n=1}^{N} |\alpha_n|^2 = 1 \quad , \tag{104}$$

but for continuous states we have

$$\langle x | \psi \rangle = \delta(x - x') \quad , \tag{105}$$

and

$$P[\psi(x)] = \int_{-\infty}^{\infty} dx' \, |\psi(x')|^2 = 1 \quad , \tag{106}$$

To obtain a real-valued probability from continuous states, one must integrate over the inner product. Therefore, when we have considered a node on a single sub-circuit, that is like a the discrete states of standing waves in that circuit. The two sub-circuits meeting at a node is like the problem of continuous states. We have two different interpretations for $\{\hat{i}, \hat{\Phi}, \hat{2}, \hat{\pi}\}$: they can be sites or vectors pointing between sites, and we have two different types of states: those from discrete and continuous spectra. When we get a continuous state that needs an extra integration step, we can remove any residual phase by integrating over a leg of the relevant sub-circuit. Fo inner products like equation (102) we can give dx' a quaternion phase $-\mathbf{k}$ such that equation (106) becomes

$$P[\psi(x)] = \int d\mathbf{x}' \, \langle \psi; \mathbf{j} | \psi; \mathbf{i} \rangle \tag{107}$$

$$= - \int dx' \, \mathbf{k}\mathbf{k} \, |\psi(x')|^2 \tag{108}$$

$$= 1 \quad . \tag{109}$$

When we use $dx \to -dx\,\mathbf{k}$, that tells us the we are integrating along the length a segment of the sub-circuit associated with $\mathbf{k}$. One expects that the integral over the length of the leg should generate the qubit which lives at the end of leg, or at least contribute to it. Additionally, we would want to rewrite the limits of integration such that they reflect the length of the relevant leg of the time circuit. It would be prudent to squeeze the Hopf fibration such that the lengths between nodes align with the values of the non-unit quaternions. However, these are only the formulae for obtaining probabilities. When a $\mathbf{i}$-state and a $\mathbf{j}$-state meet at a node, it is fine if there is a continued propagation as a $\mathbf{k}$-state, without integration over $dx\,\mathbf{k}$. Furthermore, when we get rid of the quaternion phase to give a real probability in a node, we might equally well get rid of the quaternion phase to give purely imaginary time radiation which leaves the sub-circuits to fill the bulk.

What about the triple product? We can't implement a three vector inner product but we can implement a commutative triple product. Just like the case to two waves from a single sub-circuit meeting a node, the triple product will get rid of the quaternion phase. When the quaternion phase accumulates to give a real number ± 1, the wavepacket can no longer propagate in the Hopf time circuit because each sub-circuit is phase locked to one of the three quaternion phases. These wavepackets can annihilate to produce a value at a node, or they could radiate into the bulk.

Now consider the structure of the Hopf fibration. The parallels are all circles but there is a meridian that points outward and a few hypermeridians that do so. We will want to associate the path of maximum action [25] with the legs extending outward such that they are connected at infinity to other Hopf fibrations. All the paths along the circles, and any piecewise path which stays inside a single fibration, should satisfy the least action principle but the other legs should satisfy the most action principle [25]. Therefore, the entire Hopf fibration is like a node, and therefore the nodes of the Hopf fibration have structure which is also a Hopf fibration.

The definite result of this section is that the Hopf fibration is a good template on which to model the time circuit. Furthermore, since the nodes and edges of the graph of our circuit have multiplectic structure, "graph" having its rigorous definition in linear algebra, we should be able to draw graphs in which the edges becomes nodes and the nodes become edges. A good constraint on the time circuit will be that both of these graphs are the Hopf fibration.

ELECTRICITY

Whatever the physical laws are, excepting certain cases of potential octonions, they will be crunched with the tools of matrix algebra because quantum mechanics is a linear theory. This means that every object can be represented as a matrix without regard for the representation we use to show its relationships. Therefore, we will consider the linear analysis of a primitive electrical circuit and then discuss the requirements for the construction of an analogous time circuit.

According to Strang [28], the fundamental problem of not just linear algebra, but all of applied mathematics, is

$$\left(A^T C A \right) \vec{x} = \vec{f} \quad . \tag{110}$$

Indeed, $\vec{f}$ is very much like the fifth piece of an ontological algebra of $\{\hat{i}, \hat{\Phi}, \hat{2}, \hat{\pi}; \hat{\varphi}\}$ such as that described in [29]. We will consider the case when $\vec{f} = 0$. The operator $A^T C A$ is quite like

$$\hat{M}^3 = \hat{\mathbf{u}}^{-1}\hat{H}\hat{\mathbf{u}} \ , \qquad \text{or} \qquad \hat{M}^3 = e^{-\hat{\mathbf{u}}\theta}e^{i\hat{H}t}e^{\hat{\mathbf{u}}\theta} \ , \quad (111)$$

and we make the MCM problem slightly more complex than the fundamental problem when we make the extension to

$$\hat{M}^3 = \hat{\mathbf{u}}_1^{-1}e^{i\hat{H}t}\hat{\mathbf{u}}_2 \ . \tag{112}$$

Now we have noted in passing that $\hat{M}^3$ is quite like the fundamental operator of applied mathematics and we will henceforth focus on the form A^TCA as relates to the applied problem in electricity.

Consider the electrical circuit in figure 12. The rules for describing graphs with linear algebra require a matrix A with as many rows as there are edges in the graph and as many columns as there are nodes. For our example, A is 5×4. The physical problem we will examine is the one where $\vec{x}$ gives the potential at each node and $\vec{y}$ gives the electrical current along each edge. By inspection, A is

$$A = \begin{pmatrix} -1 & 1 & 0 & 0 \\ 0 & 1 & -1 & 0 \\ 1 & 0 & -1 & 0 \\ -1 & 0 & 0 & 1 \\ 0 & 0 & -1 & 1 \end{pmatrix} \ . \tag{113}$$

Each row represent an edge. If the edge points out of a node we write -1 and if it points into a node we write 1, and 0 otherwise. To obtain the potential difference between nodes, we compute

$$A\vec{x} = V. \tag{114}$$

To get the current, we use Ohm's law $V = IR$ which is written in terms of the capacitance as

$$CV = I \ . \tag{115}$$

This is not enough information to solve everything. We also need to apply Kirchoff's current law which says the current entering any node must be equal to the current leaving it. This in enforced with

$$A^T I = 0 \ . \tag{116}$$

Putting it altogether, we get

$$A^T I = A^T(CV) = A^T\big[C(A\vec{x})\big] = A^TCA\vec{x} \ . \tag{117}$$

We have solved equation (110) for the case of $\vec{f}=0$. Our graph has $\vec{f}=0$ because there is no battery included in the circuit and current does not flow. The condition of non-flowing time current should be the limit of physics in

Minkowski space $\mathcal{H}$ which can be described with the least action principle. When the time current starts flowing due to a time battery, then that should involve maximum action paths across hyperspacetime, out of spacetime.

Now we have solved one complete physics problem, albeit a static one. If we added batteries and components then we would get systems of differential equations that have exact analogues in classically mechanical systems when the capacitance or the inductance is like mass, the current is like force or velocity, *etc.* Therefore, we will consider an unpowered time circuit under the assumption that $\vec{f}\neq0$ can be added later.

The electric current is a scalar but the time current is spinor-valued so the edges of our graph would have two arrows, perhaps a red one and a blue one. That covers the edges, what about the nodes? If x is the potential at the node in the electrical circuit then it should be the time at the node of time circuit. Positive charges want to move to lower electrical potential and world-sheets with positive time arrows want to move to higher time so there is a good analogy between time and potential. That's $\vec{x}$ and $\vec{y}$, what about A? Our construction of A will necessarily be much more complicated than the A devised here for figure 12. Not only do we need to have the spinor piece, we have the quaternion phase along the edges and at the nodes. This indicates a likely 3-plet for each node, possibly one for each level of $\aleph$ in the hyper-complex limit. The MCM concept of time is preserved when $t_\star$ exists in the nodes and $t_\pm$ exist along the edges.

What should be our analogue of Ohm's law? In the electrical problem, the capacitance matrix acts on the potential difference vector which becomes the δt vector in the time circuit. Usually time differences show up in quantum mechanics via the unitary evolution operator $e^{i\hat{H}\delta t}$ so this step would likely involve an exponential map between permutations of equations (111). When one applies the exponential map, one performs an operation like wrapping the time axis of Minkowski space
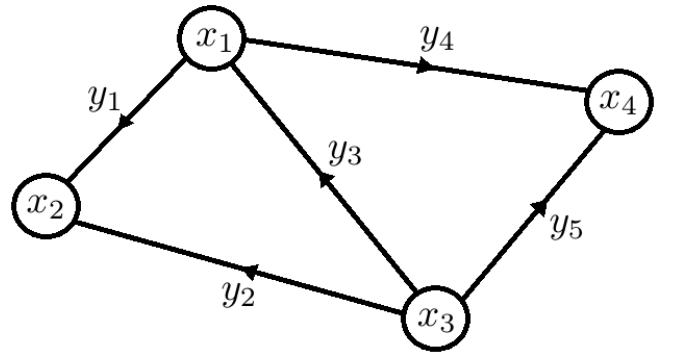

FIG. 12. This figure shows an ungrounded, unpowered electrical circuit consisting of four nodes and five edges. This circuit is like that in figure 1 with added nodes that can attach to the exterior time circuit, as in figure 8. Some of the arrows are reversed on some edges with respect to figure 1 because the time circuit has to have spinor-valued edges between multiplectic nodes.

around a cylinder [1, 13] with $x^0 \to e^{ix^0}$. Therefore, if we act on the δt vector with $\hat{H}$ and then wrap the time axis around a cylinder we will obtain the unitary evolution operator

$$\hat{H}\delta t \quad \longrightarrow \quad e^{-i\hat{H}\delta t} \quad \equiv \quad \hat{U} \quad . \tag{118}$$

Instead of the electrical currents $\vec{y}$, we would likely use the unitary evolution operator to determine the probability current. Since our electrical circuit has no batteries or parts, no current flows. In analogy, we would have no probability current between nodes and everything in $\mathcal{H}$ would stay in $\mathcal{H}$. If we added some batteries and parts to the electrical circuit then there would be a dynamical current and the time circuit would have non-vanishing probability currents among the nodes which are like $\{\mathcal{H}_1, \Omega, \varnothing, \aleph, \mathcal{H}_2\}$ in the unit cell.

How about the final part: the temporal balance equation to act as the analogue of Kirchoff's current law? The electrical nodes in figure 12 are unitary in nature, their labels are like unit vectors $\hat{x}_j$. When the time nodes are $\hat{\pi}$-, $\hat{\Phi}$-, $\hat{2}$-, and $\hat{i}$-sites, the labels will modify the magnitudes of the spinor time currents going into and coming out of each node. Furthermore, where an electrical circuit has to be physical everywhere, we add a lot of new phase structure with quaternion waves in the real and imaginary sectors so the time circuit might not exhibit the same global coherence seen in the primitive electrical circuit. The time circuit probably does not have to be physical along the legs extending past a certain level of $\aleph$ with respect to that of $t_\star$. Indeed, when the independent part of a given graph is loosely defined as the part with no loops, $t_\star$ should be exactly that part of the time circuit's graph which is constrained not to be a loop. Therefore, the time circuit should be such that everything is a loop except for one real part $t_\star \equiv x^0$ and one imaginary part $t_\star \equiv \chi^5$. This non-loop part must be the independent time arrow spinor we have used to demonstrate $\hat{H}_{\text{MCM}}$.

QUATERNIONS

If our three unit quaternions $\{\mathbf{i}, \mathbf{j}, \mathbf{k}\}$ propagate on the time circuit then we might also add imaginary quaternions so that our timewaves can go off-shell, into the bulk, which could be the exterior bulk or the interior, hypercomplexly infinitesimal bulk within each node. Imaginary quaternions are not strictly required to study the bulk because we can go off-shell with i alone but the imaginary quaternions are required for self-similarity in the fields. Consider the general solution to everything in quantum mechanics

$$\Psi = Ae^{i(\omega t - kx)} + Be^{-i(\omega t - kx)} \quad . \tag{119}$$

We have the option to add quaternion phase by replacing the i with a quaternion, or we might multiply it with a quaternion. For example, consider

$$\Psi' = Ae^{i(\omega t - kx)} + Be^{-i(\omega t - kx)} + ...$$
$$... + Ce^{i\mathbf{u}_1(\omega t - kx)} + De^{-i\mathbf{u}_2(\omega t - kx)} \quad . \tag{120}$$

We might even consider $\mathbf{u} \to \mathbf{q}$ such that a fifth component beyond i and $\mathbf{u}$ is added. Since quaternions do 4D rotations, the Lorentzian O(1,3) topology of our 4D spacetime defines a time arrow which acts as an object being rotated in 4D, and 3-spaces are rotated by their orientation with respect to these time arrows. Thus far, we have mostly considered unit quaternions but the MCM is a non-unitary model. We want to define a quaternion algebra for the ontological basis $\{\hat{i}, \hat{\Phi}, \hat{2}, \hat{\pi}\}$ [21, 26] but $\hat{i}$ is not allowed because the quaternions all have real coefficients while $\hat{i}$'s coefficient in

$$\hat{1} = \frac{1}{4\pi}\hat{\pi} - \frac{\varphi}{4}\hat{\Phi} + \frac{1}{8}\hat{2} - \frac{i}{4}\hat{i} \quad , \tag{121}$$

is imaginary. This is a hard constraint that $\{\hat{i}, \hat{\Phi}, \hat{2}, \hat{\pi}\} \not\equiv \mathbb{H}$. Furthermore, if the ontological resolution of the identity was a quaternion relationship $\hat{1} \to \mathbf{q}$ then the identity would be on the RHS because the identity is a required element of $\mathbb{H}$. To resolve these issues, consider

$$\mathbf{q}_\pi = c_{\pi_0}\hat{\pi}^0 + c_2\mathbf{2} + c_\Phi\mathbf{\Phi} + c_{\pi_1}\mathbf{\pi} \quad , \tag{122}$$

and

$$\mathbf{q}''_\Phi = c_{\Phi_0}\hat{\Phi}^0 + c_2\mathbf{2} + c_{\Phi_1}\mathbf{\Phi} + c_\pi\mathbf{\pi} \quad . \tag{123}$$

Since $\hat{i}$ does not invoke an imaginary coefficient, either of the above are perfectly valid sets of quaternions. Therefore, where have raised the issue with $\hat{i}$ when attempting to construct two sets of quaternions by splitting the 2 in $\{\hat{i}, \hat{\Phi}, \hat{2}, \hat{\pi}\}$ to make two sets of four pseudo-quaternions[26], now we have constructed two sets of rigorous quaternions without reference to $\hat{i}$. To distinguish $\mathbf{q}_\pi$ and $\mathbf{q}''_\Phi$, and to make $\mathbf{q}'_\Phi$ merely a pseudo-quaternion, consider

$$\mathbf{q}'_\Phi = -ic_{\Phi_0}\hat{\Phi}^0 + c_2\mathbf{2} + c_{\Phi_1}\mathbf{\Phi} + c_\pi\mathbf{\pi} \quad . \tag{124}$$

$\mathbf{q}'_\Phi$ has the property

$$\mathbf{2\Phi\pi} = 2\Phi\pi\mathbf{ijk} = -\Phi 2\pi\hat{1} \tag{125}$$

so the triple product is like $\hat{\pi}^0$ in both of $\{\mathbf{q}_\pi, \mathbf{q}'_\Phi\}$ because $\hat{\Phi}^0$ has an imaginary coefficient. Therefore, $\mathbf{q}_\Phi$ is injective onto $\mathbf{q}_\pi$ but not bijective. Therefore, $\mathbf{q}'_\Phi$ is not a group and group theory does not apply.

The quaternions and the Pauli matrices are related by

$$\hat{\mathbf{u}} \quad \longleftrightarrow \quad -i\vec{\sigma} \; , \qquad \text{and} \qquad \hat{1} \quad \longleftrightarrow \quad \hat{\sigma}_0 \; , \quad (126)$$

and, as in equation (48), we want to supplement that with pseudo-quaternions such that

$$\mathbf{q}'_\mu \quad \longleftrightarrow \quad -i\hat{\sigma}_\mu \; . \quad (127)$$

Indeed, if we are trying to consider every possible phase combination. which was the intention in equation (48), then why not define a totally phase-inverted pseudo-quaternion which satisfies

$$\hat{\mathbf{u}}' \quad \longleftrightarrow \quad \vec{\sigma} \; , \qquad \text{and} \qquad \hat{1}' \quad \longleftrightarrow \quad -i\hat{\sigma}_0 \; ? \quad (128)$$

To that end, consider a complex pseudo-quaternion

$$\mathbf{q}_z = \mathbf{q}_\pi + i\mathbf{q}_\Phi \; , \quad (129)$$

where

$$\mathbf{q}_\pi = c_{\pi_0}\hat{\pi}^0 + c_{\pi_2}\mathbf{2}_\pi + c_{\pi_\Phi}\mathbf{\Phi}_\pi + c_{\pi_1}\boldsymbol{\pi}_\pi \; , \quad (130)$$

and

$$-i\mathbf{q}_\Phi = c_{\Phi_0}\hat{\Phi}^0 + c_{\Phi_2}\mathbf{2}_\Phi + c_{\Phi_1}\mathbf{\Phi}_\Phi + c_{\Phi_\pi}\boldsymbol{\pi}_\Phi \; , \quad (131)$$

with all $c \in \mathbb{R}$. $\mathbf{q}_\Phi$ should satisfy the isomorphism with the Pauli matrices specified by relationships (128). When $\mathbf{q}_\pi$ has a real phase with respect to the imaginary phase of $\mathbf{q}_\Phi$, we can use those imaginary quaternions to describe the matter-energy in the foliated 3-spaces [1] that propagate along the edges of the time circuit. These are the spacelike sectors of the universes whose time axes define the time circuit. The purpose of all this added nuance will be so that the quaternion phase cannot be converted into unit Pauli matrices in all cases, but rather only under certain phase conditions defined by the c that appear in the many equations. For the purposes of physics, before one surveys all possible combinations of complex and quaternion phase, one would examine the MCM Hamiltonian and add phase as needed when it bumps into a dead end.

To distinguish $\mathbf{q}^\pi$ and $\mathbf{q}^\Phi$, consider that we have associated the entrance leg into the bounce complex with $\hat{\sigma}_0 \equiv \hat{1}$. What kind of cosmological lattice site is this? In general, we have a strong case for the input leg being a $\hat{\pi}$-site, meaning $\hat{\sigma}_0 \equiv \hat{\pi}^0$, because $\hat{M}^3$ takes input from one $\hat{\pi}$-site and returns an output at the next $\hat{\pi}$-site, which is two levels of $\aleph$ higher than the input. However, the input leg of the bounce complex is also on the finite tier of infinitude which makes a strong case for the identification $\hat{\sigma}_0 \equiv \hat{\Phi}^0$ but the $\mathbf{q}^\pi$ and $\mathbf{q}^\Phi$ quaternions have different relationships with the Pauli matrices. Figure 13 shows how we can accommodate either representation and respect the transition rule that one type of site has to go

another type on an adjacent level of $\aleph$. This figure shows the hypercomplex contour between adjacent levels of $\aleph$ developed in [10]. To the left of the figure, we start at $\hat{\pi}^0$ and then we leave the real line at $\hat{i}$. We go through $\varnothing$ at $\hat{2}$. If we were doing a closed contour on a single level of $\aleph$ then $\hat{\pi}$ marks reentry to the real line at the end of a contour integral across π radians at complex infinity. Since the selection rule says $\hat{\pi}$ can't go to $\hat{\pi}$ on the next level of $\aleph$, we finish at $\hat{\Phi}$. To the right of the figure, we start at $\hat{\Phi}^0$ and then $\hat{i}$ once again kicks the contour off the real line. The path gets to $\hat{\Phi}$ where the path on the right gets to $\hat{\pi}$. This will indicate the changing level
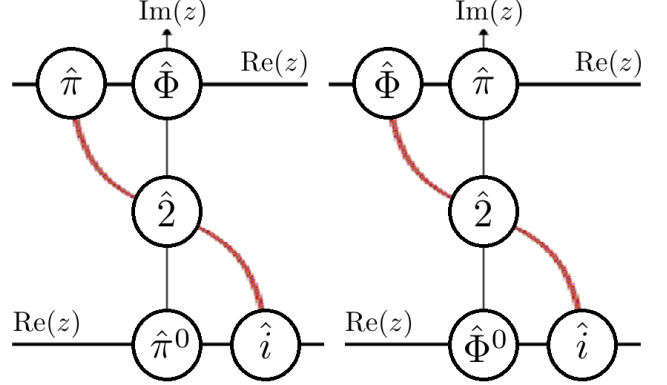
FIG. 13. This figure, adapted from [10], shows how we might take either of $\{\hat{\pi}^0, \hat{\Phi}^0\}$ as the identity quaternion. The red path is an open contour in the hypercomplex plane, one equivalent to a closed contour in the complex plane. The two modes should define chirological versus chronological evolution from one level of $\aleph$ to the next.
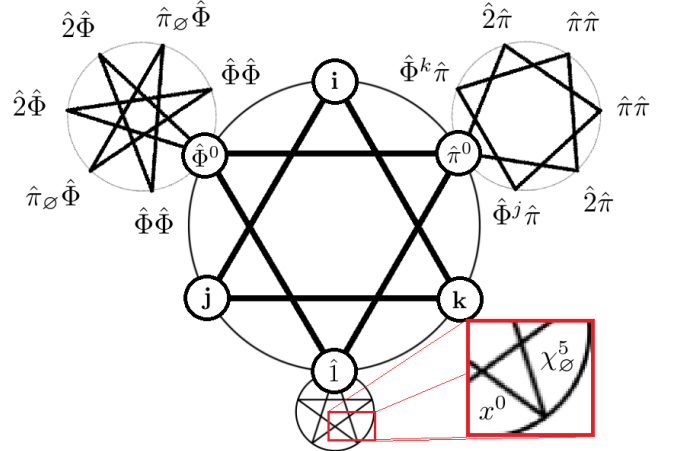
FIG. 14. This figure, adapted from [20], shows via its seven-pointed stars how $\{\hat{\pi}^0, \hat{\Phi}^0\}$ can transition into six other sites. We have a selection rule which says a site may transition to any of the other three types of sites on either of two levels of $\aleph$, and $3 \times 2 = 6$. The smaller star beyond $\hat{\Phi}^0$ demonstrates how $\mathbf{q}'^\Phi$ is injective onto $\mathbf{q}^\pi$. The two triangles represent the real and imaginary quaternions: any two corners gives a third according to the antisymmetric relationship $\varepsilon_{ijk}\mathbf{ij} = \mathbf{k}$.

of ℵ before settling into the $\hat{\pi}$-site. Both contours pass through three nodes meant to demonstrate an accumulation of quaternion phase inside the $\hat{i}$ complex phase channel.

Consider figure 14. In this time circuit schematic, The five and six pointed stars are inherited from the dodecahedral symmetry which is inherent to physics [20]. The two seven-pointed stars which complexify the dodecahedral graph represent $\hat{\pi}^0$ and $\hat{\Phi}^0$ connected to six other sites: the $\{\hat{2}, \hat{\Phi}, \hat{\pi}\}$-sites on two levels of ℵ. The two seven-pointed subcircuits represent the quaternions $\mathbf{q}^\pi$ and $\mathbf{q}^\Phi$. The injectivity of $\mathbf{q}^\Phi$ onto $\mathbf{q}^\pi$ is represented with the second, nested star beyond $\hat{\Phi}^0$, which is likely $\hat{\pi}_\varnothing$ indicating that we have moved from a closed topology to an open one by truncating information at infinity. If we reconstructed the diagram around the embedded, smaller star on the left then that would describe, likely, the circuit on another level of ℵ.

NEGATIVE FREQUENCY RESONANT RADIATION

The initial discovery of negative frequency resonant radiation, figure 15, was reported [30] two months after we first proposed the MCM negative time mode[1]. Frequency is inverse time so t_- and the new optical mode reported in [30] are likely pieces of the same puzzle. Quantum optics a natural home for the principles developed here because the photon or photonic soliton propagating in an optical fiber is a problem like the plane waves we have considered in the time circuit. One would simply substitute the "wires" for fibers and then the electrical problem becomes an optical one. Indeed, while the on-shell photon is a spin-1 boson, the elimination of one of its three polarization states due to the massless gauge invariance makes it amenable to analysis with two-component spinors. The vector properties might be extracted from the spinor via sampling two components of bispinor: one vector component from each of two spinors. In this way, would obtain one vector photon from two spinor "photons." Even while the spinors don't transform as vectors, it is possible that two of their components do, or even both when two 2D photonic state vectors are assembled from the components of two 2D spinors. Before detailing the negative time application in quantum optics, note that the MCM predicts new spin-1 particles [31] in addition to the negative time mode reported in [1, 13]. Regarding the spin of the particle discovered at CERN in 2012, they still have not reported its spin. Particle Data Group writes the following about the spin of the Higgslike particle [32], the Higgs boson having spin-0:

> "The observation of the signal in the [*two photon*] final state rules out the possibility that the discovered particle has spin 1, as a consequence of the Landau-Yang theorem.

This argument relies on the assumptions that the decaying particle is an on-shell resonance and that the decay products are indeed two photons rather than two pairs of boosted photons, which each could in principle be misidentified as a single photon."

The case in which spin-1 is not yet ruled out is astonishingly like the case developed here. Therefore, one would seek to describe the presently considered spinor states as pairs of boosted photons. Furthermore, one would would scan for pairs of boosted photons in quantum optical applications. The authors of [33] describe how it is, "possible to Lorentz-boost the particle at rest to its infinite-momentum or massless state," and that is likely what we have done with conformal coordinates in [10] and here when we freeze time by taking unit 3-velocity.

Regarding negative frequency resonant radiation, only two months after we proposed the negative time mode in [1], Rubino *et al.* wrote [30],

> "[*T*]o date only the positive branch of the dispersion has been considered when this actually also has a branch at negative frequencies. This branch is usually neglected or even considered meaningless when, in reality, it may host mode conversion to a new frequency. The fact that a mode on the negative branch of the dispersion relation may be excited [*(which is the main the result of [30])*] has a number of important implications, beyond the simple curiosity of the effect itself."

It is likely that the seemingly unphysical modes on the negative branch can be made ordinarily physical when quaternion phase accrues in that channel as

$$\mathbf{ijk} = -1 \quad , \qquad \text{and} \qquad \mathbf{i}^2 = \mathbf{j}^2 = \mathbf{k}^2 = -1 \quad . \quad (132)$$

Indeed, we will show that the scale of the energy shift between the positive and negative resonant modes [30] is on the order of the energy shift between $E_{\text{MCM}}^{\Sigma^\pm}$. The scale of the ratio of the MCM energies in $\Sigma^\pm$ is *exactly* the scale of the measured effect on the negatively signed optical mode [30], as in figure 15.

The first equation given by Rubino *et al.* is

$$k(\omega_{\text{RR}}) - k(\omega_{\text{IN}}) - \frac{(\omega_{\text{RR}} - \omega_{\text{IN}})}{v} - K_{\text{NL}} = 0 \quad . \quad (133)$$

This is a wave-vector conservation relation. In the section on electricity we derived a requirement for some conservation law which be the time circuit analogue of Kirchoff's current law and equation (133) is just that sort of law. Where Rubino *et al.* show the wavenumber (vector) as a function of the angular frequency, we have written ω as a function of k when examining the chronological and chirological evolutions under $\hat{H}_{\text{MCM}}^{\Sigma^\pm}$.
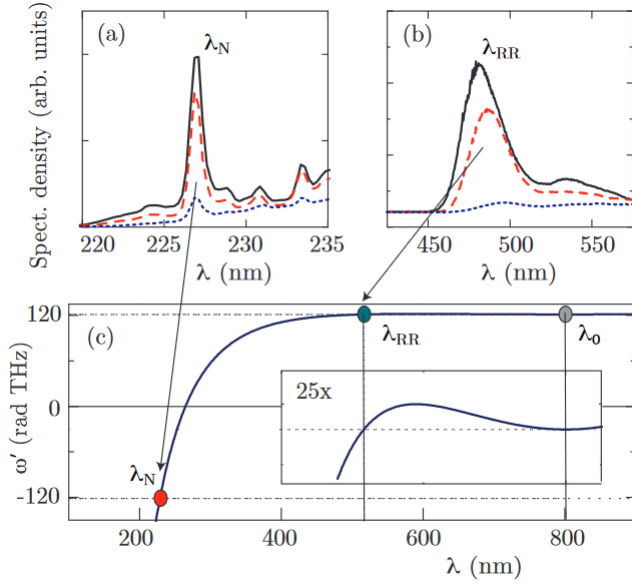
FIG. 15. This figure from [30] shows a resonant peak λ_{RR} and also a newly discovered negative resonant peak λ_{N}. Since frequency is inverse time, this optical mode is evidence of the existence of the MCM's spin-down time spinor mode. The fine structure of three or four modes in the λ_{N} peak versus one pseudo-Gaussian peak for λ_{RR} on the right is indicative of the fine structure that we would assemble with the MCM site transition rule: one site in λ_{RR} versus decomposition into three or four sites in λ_{N}. Four peaks would represent the totality of the sites and three would represent the transition rule.

v in equation (133) refers the the velocity of the waves inside the fibers. In free space $v = c = 1$, so v is a unit velocity in free space but electromagnetic waves slow down inside matter giving $0 < v < 1$. When we take the waves out of the fibers, they speed up to $v = 1$. When we take them out of the universe, into the bulk of the MCM unit cell, they will speed up even more so that their velocities are over-unity. (We have shown that propagation across the unit cell must be faster than light in [26].) Therefore, the applicability of the MCM principles to the quantum optical application is self-evident: waves going into spacetime from hyperspacetime are like waves going into fibers from the free space.

Regarding equation (133), Rubino *et al.* write [30],

> "ω_{IN} and ω_{RR} are the soliton and [*resonant radiation*] frequencies, v is the soliton velocity, [K_{NL}] is a nonlinear correction term that may be small or even negligible at low intensities[.] A very similar process occurs also in bulk media. The stationary 1D fibre soliton is now replaced by the stationary 3-dimensional X-wave."

X-waves are waves that travel in a direction at constant velocity. Therefore, a 3D X-wave describes a configuration like the intersection of parallels, meridians, and hypermeridians in which each is type of fiber with

its own index of refraction and waves travel along each type of fiber with constant velocity. We expect that the constant velocities along the 3D time circuit X-wave will be faster than light velocities $v \in \{2, \Phi, \pi\}$ in units where $c = 1$. By replacing the unit quaternions in E_{MCM} with over-unity ontological quaternions and using them as analogue velocities in the bulk of the MCM unit cell, we will speed up the "spinor photons" in hyperspacetime.

Table I shows data from [30] in its two left columns: the measured wavelengths of the resonant and negative resonant modes. On the right, the table shows energy shift between positive and negative resonant modes and the ratio of energy shift to the energy each mode. Now we will examine the ratio of the MCM energies in $\Sigma^{\pm}$ and show that they are on the correct scale to give the observed energy shift between the resonant and negative resonant quantum optical modes. The MCM energy derived for Σ^{+} is

$$E_{\mathrm{MCM}}^{\Sigma^{+}}(\phi_{+}; \hat{\mathbf{u}}_1, \hat{\mathbf{u}}_2) = \frac{1}{2} \left| \hat{\mathbf{u}}_1 \phi_{+} \hat{\mathbf{u}}_2 \right| , \qquad (134)$$

and it follows that we would find

$$E_{\mathrm{MCM}}^{\Sigma^{-}}(\phi_{-}^{2}; \hat{\mathbf{u}}_1, \hat{\mathbf{u}}_2) = \frac{1}{2} \left| \hat{\mathbf{u}}_1 \phi_{-} \hat{\mathbf{u}}_2 \right| . \qquad (135)$$

The ratio we will compute is

$$\Delta E_{\mathrm{MCM}}(\phi_{\pm}) \quad \equiv \quad \frac{E_{\mathrm{MCM}}^{\Sigma_2^{-}}(\phi_{-}; \hat{\mathbf{u}}_1^{-}, \hat{\mathbf{u}}_2^{-})}{E_{\mathrm{MCM}}^{\Sigma_1^{+}}(\phi_{+}; \hat{\mathbf{u}}_1^{+}, \hat{\mathbf{u}}_2^{+})} . \qquad (136)$$

The goal in calculating ΔE_{MCM} is to compare it to the empirical $\Delta E / E_{\mathrm{RR}}$ data [30]. We will take the energy in Σ_1^{+} as the resonant energy and then suppose that the energy shift of the negative mode is derived from a phase alignment in the time circuit which dumps the energy of

λ_{RR} (nm)	λ_{N} (nm)	ΔE (eV)	$\Delta E / E_{\mathrm{RR}}$	$\Delta E / E_{\mathrm{N}}$
542	233.1	3.032	1.325	0.570
542	232.1	3.055	1.335	0.572
526	227.0	3.105	1.317	0.568
478	218.1	3.091	1.192	0.544
480	218.9	3.081	1.193	0.544
	avg.	3.073	1.272	0.560

TABLE I. The two leftmost columns contain resonant radiation data taken from [30]. λ_{RR} is the wavelength of a resonant mode and λ_{N} is the wavelength of the corresponding negative resonant mode. Using $E = hc/\lambda$ and $hc = 1240 \, \mathrm{eV \cdot nm}$, we calculate the energy difference between the resonant mode and the negative resonant mode. The final columns show the ratio of the energy shift to the resonant and negative resonant energies.

Σ_2^- into the negative mode. In this way, $E_{\text{MCM}}^{\Sigma_2^-}$ is something that we can compare with ΔE in the experimental data. To be clear, we use ΔE_{MCM} to examine the case in which one hundred percent of the extra energy of the negative mode comes from Σ_2^-. We know what to do about the unit quaternions that appear in ΔE_{MCM} but what about the fields $\phi_\pm$? The only characteristic values that we have for $\phi_\pm$ are derived from

$$\phi_\pm^2(\chi_\pm^5) = \chi_\pm^5 \quad . \tag{137}$$

On Ω, we have $\chi_+^5 = \Phi$ and we have $\chi_-^5 = -1$ on $\aleph$ [6]. Therefore, we will compute the ratio of the energies on Ω and $\aleph$, before and after the waves cross the singularity $\varnothing$

When a wave from free space in the universe goes into a fiber it slows down. When a wave leaves the universe $\mathcal{H}$ to go to Ω, one or both of the unit quaternions in its energy function needs to go over-unity. When we have two quaternions input to $\varnothing$ from Σ_1^+ we will get two other quaternions out in Σ_2^- (via the Pauli matrix bounce permutations) so we will consider two arbitrary quaternions for the Σ_2^- energy. After we consider the case when the energy depends on the linear field $\phi_\pm$, we will also examine the quadratic dependence with

$$E_{\text{MCM}}^{\Sigma^\pm}(\phi_\pm^2; \hat{\mathbf{u}}_1^\pm, \hat{\mathbf{u}}_2^\pm) = \frac{1}{2}\left|\hat{\mathbf{u}}_1^\pm \phi_\pm^2 \hat{\mathbf{u}}_2^\pm\right| \quad . \tag{138}$$

First, we will examine the simplest route which leaves $\mathcal{H}$ as the case in which one unit quaternion in Σ^+ is replaced with $\boldsymbol{\Phi}$. The MCM convention is such that $\hat{\Phi}$ is associated with Ω and that is the first case we will consider. For further simplicity, we will first consider the case when $\boldsymbol{\Phi}$ is preserved in Σ_2^- but $\hat{\mathbf{u}}_2^+$ gets converted to one of $\{\mathbf{2}, \boldsymbol{\Phi}, \boldsymbol{\pi}\}$. The numerical values are

$$\frac{E_{\text{MCM}}^{\Sigma_2^-}(i; \boldsymbol{\Phi}, \mathbf{2})}{E_{\text{MCM}}^{\Sigma_1^+}(\sqrt{\Phi}; \boldsymbol{\Phi}, \hat{\mathbf{u}}_2^+)} = 1.572 \tag{139}$$

$$\frac{E_{\text{MCM}}^{\Sigma_2^-}(i; \boldsymbol{\Phi}, \boldsymbol{\Phi})}{E_{\text{MCM}}^{\Sigma_1^+}(\sqrt{\Phi}; \boldsymbol{\Phi}, \hat{\mathbf{u}}_2^+)} = 1.272 \tag{140}$$

$$\frac{E_{\text{MCM}}^{\Sigma_2^-}(i; \boldsymbol{\Phi}, \boldsymbol{\pi})}{E_{\text{MCM}}^{\Sigma_1^+}(\sqrt{\Phi}; \boldsymbol{\Phi}, \hat{\mathbf{u}}_2^+)} = 2.470 \quad . \tag{141}$$

Equation (140) yields exactly $\Delta E/E_{\text{RR}}$ avg., which is derived from the measured, not predicted, values given in [30]. This result is tantalizing but the negative resonant effect is nonlinear while we consider only $\Delta E_{\text{MCM}} \sim E^1/E^1$. This tight agreement, therefore, may or may not be incidental. What is hardly incidental is that the scale of the linear MCM effect is on the scale of the observed effect which includes small nonlinear contributions. Equation (141) is not in the ballpark of $\Delta E/E_{\text{RR}} = 1.272$ so let us consider a non-unit quaternion of length $\pi/2$ instead. In this picture, one envisions

the $\hat{\Phi}$ object anchored in the center of a length of π so that two lengths of $\pi/2$ result. Indeed, in this research program we have consistently compared the length Φ to the length $\pi/2$ but we have not made many points regarding the lengthlike congruency of Φ and π. For instance, in [10], we used $\hat{\Phi}$ to point beyond infinity when infinity was located at the origin of $\widetilde{y}_+ \in (-\pi/2, \pi/2)$. The operative principle was that Φ is just greater than $\pi/2$, not that it is significantly smaller than π. If we get $\pi/2$ by splitting π in half, then π is like chiros $\chi_\pm^5$ and that leaves chronos x^0 to be like Φ which is the opposite interpretation to what we have used previously. When we compute ΔE_{MCM} with $\pi/2$ we get

$$\frac{E_{\text{MCM}}^{\Sigma_2^-}(i; \boldsymbol{\Phi}, \boldsymbol{\pi}/2)}{E_{\text{MCM}}^{\Sigma_1^+}(\sqrt{\Phi}; \boldsymbol{\Phi}, \hat{\mathbf{u}}_2^+)} = 1.235 \quad . \tag{142}$$

This is also very close to $\Delta E/E_{\text{RR}}$. The average of the $\{\mathbf{2}, \boldsymbol{\Phi}, \boldsymbol{\pi}/2\}$ energy ratios is 1.360. Since we have neglected any nonlinear effects while the authors of [30] describe a nonlinear effect, this 6.9% disagreement of our average with $\Delta E/E_{\text{RR}}$ looks good and the 0.000% disagreement of equation (140) looks very good.

Before moving on to consider the quadratic fields, we will note some significant numbers. Equation (139) tells us that

$$\frac{2}{\sqrt{\Phi}} \approx \frac{\pi}{2} \quad , \qquad \text{with} \qquad \Delta\aleph = 0.01\% \quad . \tag{143}$$

Furthermore, all of the energy shifts ΔE in table I are approximately equal to π. One would expect π to only show up in dimensionless relationships, so this too may be incidental, but we find that

$$\Delta E \text{ avg.} \approx \pi \quad , \qquad \text{with} \qquad \Delta\aleph = 2.2\% \quad . \tag{144}$$

It has been a recurring theme in the MCM that π should accrue during each application of $\hat{M}^3$: either one moves from the $\hat{\pi}^0$-site in $\mathcal{H}_1$ to the $\hat{\pi}^1$-site in $\mathcal{H}_2$, or a co-$\hat{\pi}$ is joined to a second co-$\hat{\pi}$, or we apply tangent inverses such that

$$\tan'^{-1}[\tan'(\theta)] = \theta + \pi \quad , \tag{145}$$

[10]. One would explore the variations of the conformal triple tangent [10] with hyperbolic tangent and inverse hyperbolic tangent functions to distinguish the closed and open topologies of $\aleph$ and Ω, or AdS and dS. In terms of the hyperboloidal geometry inherited from the embedding in $\Sigma^\pm$, we need to accommodate the distinct hyperboloids of one and two sheets for AdS and dS spacetimes [17, 27]. Likely, there is a specific variant of equation (145) which gives arbitrage of π via the arrangement of the branch and principle value definitions of the many complex-valued quaternion wavefunctions. In fact, the most complex feature of the Tipler sinusoid [14, 34], the

sinusoid being a type of timewave, is that its metric uses trigonometry functions *and* logarithms but, truly, the inverse hyperbolic trigonometry functions are defined as logarithms. Equation (145) simply demonstrates that it is possible to achieve arbitrage of π via some operation and here we add to the comments of [10] that one would explore the hyperbolic variants of the tangent and inverse tangent functions.

In the present paper, we have considered the non-relativistic limit where the asymmetry of dS and AdS did not contribute. The inclusion of hyperbolic tangent functions in equation (145) might be useful for creating smooth topological bifurcations such as those needed to smoothly distinguish the O(1,4) and O(2,3) topologies of $\Sigma^{\pm}$. We mention this in reference to the classical problem of field line breaking and reconnection because this classical mega-problem is a major theme in the overall constructive elements of the MCM and the theory of infinite complexity [17, 27]. Field line breaking and reconnection will be important in the time circuit because time radiation will be such that packets of time flux can propagate off the edges of the graphs of the time circuit. We need to break their field line connections to their sources so that they can propagate as disconnected loops of flux. Time radiation should be like gravitational radiation, and we have shown that this is an allowed mode in the bulk metric of $\Sigma^{\pm}$ [14].

The $\Delta E_{\mathrm{MCM}}(\phi_{\pm}^2)$ in table II is computed with

$$\Delta E_{\mathrm{MCM}}(\phi_{\pm}^2) \quad \equiv \quad \frac{E_{\mathrm{MCM}}^{\Sigma_2^-}(\phi_-^2; \hat{\mathbf{u}}_1^-, \hat{\mathbf{u}}_2^-)}{E_{\mathrm{MCM}}^{\Sigma_1^+}(\phi_+^2; \hat{\mathbf{u}}_1^+, \hat{\mathbf{u}}_2^+)} \quad . \qquad (146)$$

The upper part of table II shows the case when we have two unit quaternions in the denominator. None of the values in the upper part of the table are close to the measured values; 1.850 and 2.360 are not close to 1.272. When we can't have two ones in the denominator, this reflects the boundary condition in which a wave gains an over-unity velocity component in its MCM Hamiltonian when it leaves $\mathcal{H}$ via the maximum action trajectory across the MCM unit cell [25]. Noting that $1.85^2 = 1.36$, however, we might consider the case when the non-unit quaternions have magnitudes according to the squares and square roots of $\{\hat{2}, \hat{\Phi}, \hat{\pi}/2\}$. In that case the experimental scale of $\Delta E/E_{\mathrm{RR}}$ would much more closely agree with the MCM average with two unit quaternions in the denominator.

The results on the bottom of table II show the case when the energy in Σ^+ has any one non-unit quaternion, one associated with leaving $\mathcal{H}$ and going into the bulk, and then the "negative" Σ_2^- mode gains all of its energy from addition of the second non-unit quaternion in the $\aleph$-brane. The quadratic and linear averages 1.081 and 1.380 are decently close to the experimental value 1.272. Some of the configurations are right on the money, and some configurations show energy loss rather than gain from Σ_1^+ to Σ_2^-. Overall, the best fit is the Hamiltonian with the linear field and one non-unit quaternion in Σ^+.

$\mathbf{u}_1^-$	$\mathbf{u}_2^-$	$\mathbf{u}_1^+$	$\mathbf{u}_2^+$	$\Delta E_{\mathrm{MCM}}(\phi_{\pm}^2)$	$\Delta E_{\mathrm{MCM}}(\phi_{\pm})$
2	2	1	1	2.472	3.145
2	Φ	1	1	2.000	2.544
2	$\pi/2$	1	1	1.942	2.470
Φ	Φ	1	1	1.618	2.058
Φ	$\pi/2$	1	1	1.571	1.998
$\pi/2$	$\pi/2$	1	1	1.525	1.940
			avg.	1.850	2.360

$\mathbf{u}_1^-$	$\mathbf{u}_2^-$	$\mathbf{u}_1^+$	$\mathbf{u}_2^+$	$\Delta E_{\mathrm{MCM}}(\phi_{\pm}^2)$	$\Delta E_{\mathrm{MCM}}(\phi_{\pm})$
2	2	2	1	1.236	1.572
2	Φ	2	1	1.000	1.272
2	$\pi/2$	2	1	0.971	1.235
Φ	Φ	2	1	0.809	1.029
Φ	$\pi/2$	2	1	0.786	0.999
$\pi/2$	$\pi/2$	2	1	0.762	0.971
2	2	Φ	1	1.528	1.944
2	Φ	Φ	1	1.236	1.572
2	$\pi/2$	Φ	1	1.200	1.527
Φ	Φ	Φ	1	1.000	1.272
Φ	$\pi/2$	Φ	1	0.971	1.235
$\pi/2$	$\pi/2$	Φ	1	0.943	1.199
2	2	$\pi/2$	1	1.574	2.002
2	Φ	$\pi/2$	1	1.273	1.619
2	$\pi/2$	$\pi/2$	1	1.237	1.572
Φ	Φ	$\pi/2$	1	1.031	1.310
Φ	$\pi/2$	$\pi/2$	1	1.000	1.272
$\pi/2$	$\pi/2$	$\pi/2$	1	0.972	1.235
			avg.	1.081	1.380

TABLE II. The table shows the quadratic field energies with two non-unit quaternions in the numerator and one non-unit quaternion in the denominator. The values for the quadratic field are $\phi_+^2 = \Phi$ and $\phi_-^2 = -1$ and those for the linear fields are $\phi_+ = \sqrt{\Phi}$ and $\phi_- = i$.

The average in that case is 1.380 which differs from 1.272 by 8.5% but some particular modes differ by 0.000%.

Now we have demonstrated that the characteristic scale of the ratio of the energy shift to the resonant energy is also the characteristic scale of the ratio the MCM energies in $\Sigma^{\pm}$. Take careful note that we have only proposed to modify the quaternion rotations, and not the quaternions themselves by using them to modify the braket notation. By taking two non-unit quaternions in the rotation of a 4D vector, likely a timecurrent vector on the edges of the graphs of the time circuit, and which is like a time arrow in the 4D and 5D bulk due to the O(1,3) Lorentzian topology, one has

$$t'_{\star} = \hat{\mathbf{u}}^{-1} t_{\star} \hat{\mathbf{u}} \qquad (147)$$

which becomes

$$t'_\star = \{\mathbf{2}^{-1}, \mathbf{\Phi}^{-1}, \boldsymbol{\pi}^{-1}\} t_\star \{\mathbf{2}, \mathbf{\Phi}, \boldsymbol{\pi}\} \quad . \tag{148}$$

Therefore, one would use the inverse operators to model the energy shift $\Delta E/E_{\mathrm{N}}$. One notices that $\Delta E/E_{\mathrm{RR}}$ and $\Delta E/E_{\mathrm{N}}$ are not inverses of each other and this should indicate non-commutativity in the time circuit on top of the non-commutativity of the 3D rotations. In modifying the bra-ket notation, we modify the method by which we compute expectation values. We can compute expectation values for the energy by putting the Hamiltonian inside the bra-ket, so that is highly useful for studying systems of massless particles such as those resonant photons and solitons in the quantum optical application. (The semblance of the soliton and the photon is that of the electron and the hole on the electron current in the electrical application. A soliton is simply a disturbance on the electromagnetic field inside the fiber; it is an equivalent notation, and reflects the duality of the descriptions of electricity via the motions of electrons in direction or holes in the current moving in the opposite direction.)

Note the special case in the linear formulation

$$\frac{E_{\mathrm{MCM}}^{\Sigma_2^-}(-1; \boldsymbol{\pi}/2, \mathbf{\Phi})}{E_{\mathrm{MCM}}^{\Sigma_1^+}(\mathbf{\Phi}; \mathbf{\Phi}, \hat{\mathbf{u}}_2^+)} = 0.971 \quad . \tag{149}$$

This is the greater of two modes of energy loss. It is derived from the case in which Φ is just larger than $\pi/2$. It is this property of Φ that allows us to use $\hat{\Phi}$ to point to a topological singularity beyond the bounds of the extended complex plane [10]. The structure of the singularity is like a Kerr–Newman black hole [23, 35] whose ergosphere is known *not* to conserve energy in all cases. Therefore, while the obvious application of the time circuit would be to send information, or possibly even matter-energy, to nodes whose time is in the past or future, we might have a subtle effect in which we could direct energy into nodes whose time is in the present, such as the negative resonant mode. For instance, as energy tends to decrease in $\bar{U}$, if a modal connection can be established through the graph of the time circuit, $\bar{U}$'s decreasing energy might be dumped into U as increasing energy. Since equation (149) is very near the transition from energy loss to energy gain, it deserves special attention, as does the corresponding maximally dissipative quadratic field mode

$$\frac{E_{\mathrm{MCM}}^{\Sigma_2^-}(-1; \boldsymbol{\pi}/2, \boldsymbol{\pi}/2)}{E_{\mathrm{MCM}}^{\Sigma_1^+}(\mathbf{\Phi}; \mathbf{2}, \hat{\mathbf{u}}_2^+)} = 0.762 \quad . \tag{150}$$

[1] Jonathan W. Tooker. Dark Energy in M-Theory. *viXra:1208.0077*, (2009).
[2] Jonathan W. Tooker. The General Relevance of the Modified Cosmological Model, Section IV.1. *viXra:1712.0598*, (2017).
[3] Jonathan W. Tooker. The General Relevance of the Modified Cosmological Model, Section II.1. *viXra:1712.0598*, (2017).
[4] Abhay Ashtekar and Parampreet Singh. Loop Quantum Cosmology: A Status Report. *arXiv:1108.0893*, (2011).
[5] B.S. DeWitt. Quantum Theory of Gravity I. The Canonical Theory. *Phys. Rev., 160, 1113-1148*, (1967).
[6] Jonathan W. Tooker. The General Relevance of the Modified Cosmological Model, Section I.1. *viXra:1712.0598*, (2017).
[7] Jonathan W. Tooker. The General Relevance of the Modified Cosmological Model, Section II.2. *viXra:1712.0598*, (2017).
[8] Jonathan W. Tooker. On the Riemann Zeta Function. *viXra:1703.0073*, (2017).
[9] Jonathan W. Tooker. Derivation of the Limits of Sine and Cosine at Infinity. *viXra:1806.0082*, (2018).
[10] Jonathan W. Tooker. The Golden Ratio in the Modified Cosmological Model. *viXra:1807.0136*, (2018).
[11] Jonathan W. Tooker. The General Relevance of the Modified Cosmological Model, Section I.2. *viXra:1712.0598*, (2017).
[12] R. Arnowitt, S. Deser, and C.W. Misner. Note on the Positive-definiteness of the Energy of the Gravitational Field. *Annals of Physics* **11, 116**, (1960).
[13] Jonathan W. Tooker. Modified Spacetime Geometry Addresses Dark Energy, Penrose's Entropy Dilemma, Baryon Asymmetry, Inflation and Matter Anisotropy. *viXra:1302.0022*, (2009).
[14] Jonathan W. Tooker. The General Relevance of the Modified Cosmological Model, Section IV.2. *viXra:1712.0598*, (2017).
[15] Jonathan W. Tooker. The General Relevance of the Modified Cosmological Model, Section III.10. *viXra:1712.0598*, (2017).
[16] Jonathan W. Tooker. The General Relevance of the Modified Cosmological Model, Section III.8. *viXra:1712.0598*, (2017).
[17] Jonathan W. Tooker. The General Relevance of the Modified Cosmological Model, Section IV.4. *viXra:1712.0598*, (2017).
[18] Jonathan W. Tooker. The General Relevance of the Modified Cosmological Model, Section IV.8. *viXra:1712.0598*, (2017).
[19] Jonathan W. Tooker. Geometric Cosmology. *viXra:1301.0032*, (2013).
[20] Jonathan W. Tooker. Ontological Physics. *viXra:1312.0168*, (2013).
[21] Jonathan W. Tooker. The General Relevance of the Modified Cosmological Model, Section II.7. *viXra:1712.0598*, (2017).
[22] Jonathan W. Tooker. The General Relevance of the Modified Cosmological Model, Section IV.3. *viXra:1712.0598*, (2017).
[23] Jonathan W. Tooker. The General Relevance of the Modified Cosmological Model, Section II.6. *viXra:1712.0598*, (2017).
[24] Jonathan W. Tooker. The General Relevance of the Modified Cosmological Model, Section III.9. *viXra:1712.0598*, (2017).
[25] Jonathan W. Tooker. The General Relevance of the Modified Cosmological Model, Section I.3. *viXra:1712.0598*, (2017).
[26] Jonathan W. Tooker. Infinitely Complex Topology Changes with Quaternions and Torsion. *viXra:1505.0131*, (2015).

[27] Jonathan W. Tooker. The General Relevance of the Modified Cosmological Model, Section IV.5. *viXra:1712.0598*, (2017).

[28] Gilbert Strang. MIT OCW: Linear Algebra, Fall (2011). Lesson 12: Graphs, Networks, Incidence Matrices.

[29] Jonathan W. Tooker. The General Relevance of the Modified Cosmological Model, Section II.5. *viXra:1712.0598*, (2017).

[30] E. Rubino *et al.* Negative Frequency Resonant Radiation. *arXiv:1201.2689*, (2012).

[31] Jonathan W. Tooker. Quantum Structure. *viXra:1302.0037*, (2013).

[32] M Tanabashi et al. 2018 Review of Particle Physics. *Phys. Rev. D, **98**, 030001*, (2018).

[33] Sibel Baskal, Young S. Kim, and Marilyn E. Noz. Photons in the Quantum World. *arXiv:1711.09210*, (2017).

[34] Frank J. Tipler. Rotating Cylinders and the Possibility of Global Causality Violation. *Phys. Rev., **9**, 8*, (1974).

[35] Jonathan W. Tooker. Kerr-Newman, Jung, and the Modified Cosmological Model. *viXra:1405.0329*, (2014).